Lu, X.; Mohedano, M.; Blawert, C.; Matykina, E.; Arrabal, R.; Kainer, K.U.; Zheludkevich, M.L.:

Plasma electrolytic oxidation coatings with particle additions – A review

In: Surface and Coatings Technology (2016) Elsevier

DOI: 10.1016/j.surfcoat.2016.08.055

Plasma electrolytic oxidation coatings with particle additions – A review

X. Lu[a], M. Mohedano[a], C. Blawert[a], E. Matykina[b], R. Arrabal[b], K.U. Kainer[a], M.L. Zheludkevich[a,c]

[a]Helmholtz-Zentrum Geesthacht, Magnesium Innovation Centre, Institute of Materials Research, Max-Planck-Str. 1, D-21502 Geesthacht, Germany

[b]Departamento de Ciencia de Materiales, Facultad de Ciencias Químicas, Universidad Complutense, 28040, Madrid, Spain

[c]Department of Materials and Ceramic Engineering, CICECO-Aveiro Institute of Materials, University of Aveiro, 3810-193 Aveiro, Portugal

Corresponding author: Phone: +494152871943, Fax: +494152871960,

Email: xiaopeng.lu@hzg.de

Abstract

Plasma electrolytic oxidation (PEO) processing for light metals is known for decades and has been established as a well-known industrial surface treatment offering a reasonable wear and corrosion protection. However, long-term protection is compromised by the intrinsic porosity and limited range of composition in the PEO layer. A novel approach is to introduce particles to the electrolyte, aiming at their in-situ incorporation into PEO coatings during growth. The idea is that with the help of particles the defects can be sealed, and the composition range and the functionalities of produced coatings can be enhanced. So far, multifunctional coatings with anticorrosion, self-lubrication, anti-wear, bioactive and photocatalytic properties were produced with the aid of particle addition.

The properties of particle itself, together with electrical and electrolyte parameters during PEO processing determine the way and efficiency of particle uptake and incorporation into the

coatings. Normally incorporation of the particles into the coating can range from fully inert to fully reactive. This paper reviews recent progress on particle-containing PEO coatings formed on Mg, Al and Ti alloy substrates. The main focus is given to the uptake mechanism of particle into PEO layers and the introduced microstructural and functional changes.

1 Introduction

Plasma electrolytic oxidation (PEO), also referred to microarc oxidation (MAO), is a promising process derived from conventional anodizing to form ceramic-like coatings mainly on magnesium, aluminum and titanium alloys. The main advantages are enhanced wear and corrosion resistance together with other features such as improved biocompatibility, biodegradability, thermal stability and dielectric properties [1-6]. PEO usually employs eco-friendly alkaline electrolytes and the coatings are formed under a high voltage, when short-living discharges occur locally at the metal/electrolyte interface leading to a conversion of the metal to an oxide based layer. Metals or alloys are normally treated in silicate, phosphate, fluoride or aluminate containing electrolytes, resulting in coatings containing amorphous and/or crystalline phases stemming from both the substrate and electrolyte compounds. The formation mechanisms of the PEO coatings are complex due to the involvement of electro-, thermal-, and plasma-chemical reactions [1, 7].

However, high porosity, limited range of chemical compositions and high energy consumption are the main restrictions for PEO coatings to achieve a wider range of applications and desirable properties such as long-term protection or multifunctional surfaces. In general, the properties of PEO coatings rely on their microstructure and composition, which are mainly determined by the

process and electrolyte parameters. In the case of process parameters, various investigations have been performed to optimize the electrical conditions, such as applied voltage/current magnitude, mode, frequency and duty cycle [8-12]. The applied electrical parameters influence the PEO process characteristics, including the breakdown voltage and the discharge events, both in terms of discharge intensity and density, which have significant effects on the coating microstructure and properties. However, it is unlikely to avoid high porosity for PEO coatings, especially for Mg alloys, and also the coating properties are confined due to the limited influence of the electrical parameters on coating composition. Modifying the electrolyte composition is another effective way to optimize the microstructure and composition in order to improve coating properties [13-16]. Recent developments in this area are focused on the addition of particles into the electrolyte, aiming at in-situ incorporation or sealing of the porous PEO coatings, and also endowing the coatings with new functionalities. The addition of particles into the electrolyte influences the PEO processing because it can change the electrolyte, i.e. pH value, conductivity and viscosity, which might have an effect on the coating morphology and properties in return. If particles are incorporated without reaction or no new phase formation, it is considered as an inert incorporation. This means that the size and shape of the particles do not undergo noticeable change and the particles can be easily traced and identified in the layer, even if some superficial reaction may take place in the interfacial region between the particles and the coating matrix. The second possibility is reactive or partly reactive incorporation. In this case the particles can be melted by the high-energy discharges in the PEO processing and react with other components from electrolyte and matrix. This complex process depends on numerous factors, such as the substrate, the size, melting point, concentration and zeta potential of the particles, the

composition of the base electrolyte as well as the energy provided by the discharges. The present review gives a critical overview about the influence of different particles on the PEO process, the coating composition and properties on Mg, Al and Ti and their alloys.

2 Particles used in PEO coatings: characteristics and requirements

In vast majority of the studies, particles are directly added in the form of powder or sol to the electrolyte, since it is more flexible and confers more alternatives than the particles stemming from the substrate, e.g., the particle reinforcement in metal matrix composites. Additionally, in-situ particle formation can occur in the electrolyte intentionally or if the solubility limit of certain compounds is exceeded during PEO processing. Such systems can also be considered as particle-containing electrolytes. A challenge is to obtain uniform dispersion of particles in the PEO electrolyte. Zeta potential is used to evaluate the surface charge of the particles and their dispersion stability in a certain solution [17]. The magnitude of the zeta potential indicates the degree of electrostatic repulsion between the adjacent particles in the solution. Particles with higher absolute value of zeta potential are more stable, resulting in inhibiting agglomeration and settling in PEO electrolyte. A high zeta potential (absolute value) is desirable in electrophoretic process as this enhances the rate of particle movement under a given electrical field [18]. It was found that most of the particles are negatively charged and demonstrate negative zeta potential in the commonly used alkaline electrolytes. The negative zeta potential could facilitate the incorporation of particles since the substrate and the coating on top of it serves as anode during DC or positive pulses under AC conditions. In particular, the absolute value of zeta potential increases with the pH value of the PEO electrolyte (Figure 1) [19, 20]. The properties of the particles (e.g., size and density) also determine their stability in the electrolyte. For instance, it is

likely that there is a limitation of the particle size, since the majority of the studies have used particles which are less than 10 µm. Consequently, external forces are generally utilized to avoid sedimentation and agglomeration of the particles, e.g., mechanical stirring, gas bubbling, electrolyte pumping and ultrasonic agitation. In some cases, surfactants are utilized to improve dispersion stability of the particles, e.g., PTFE, MnO_2 and NiO [21, 22]. Another approach is to use in-situ formed sol suspensions during preparation of the electrolyte. However, organic solvents (e.g., ethanol) or specific complexants are often used to synthesize such sols [23-25]. They often act as unwanted additives in the electrolyte and might have an adverse effect on PEO coatings. Table 1 summarizes various particles which have been introduced to the PEO electrolyte aiming at improving the properties (corrosion and wear performance) and providing new functionalities (biocompatibility, antibacterial, ferromagnetic and catalytic activities) for PEO coatings. Thus a wide field of particles and possible applications are available.

3 Influence of particle addition on electrical response of PEO process

Generally, addition of new components into the electrolyte can have an effect on the electrical response of PEO process. It was demonstrated that addition of particles can slow down the voltage ramp during PEO treatment [17, 20, 26, 27]. Li et al. [26] reported that the voltage ramp was delayed in the presence of Al_2O_3 particles (Figure 2). Lim et al. [27] claimed that addition of CeO_2 particles in the electrolyte have decreased the final voltage for PEO processing. However, controversial results about the voltage response and final voltage were found by other researchers [28-30]. Wang et al. [29] have found that addition of Al_2O_3 nanoparticles enables PEO coatings to grow faster and reach higher final voltage. The size of the particles has an effect on the PEO processing. Nano-sized particles can facilitate faster transition of the current/voltage response

during PEO treatment in comparison to micro-sized particles [30]. It was also reported that there is no significant influence of particles addition on PEO processing [19, 31-39]. The addition of zirconia particles had only minor influence on the coating growth rate and voltage response during PEO treatment [32, 33]. This discrepancy is probably ascribed to the different power supplies and electrical parameters utilized during PEO process, as the pH and conductivity of the electrolyte are not greatly altered after particle addition. However, the addition of particles in form of alco-sol to the electrolyte has a larger influence on the electrical response of PEO process [40, 41]. This is probably caused by the main solvent of the alco-sol, ethanol, which decreases the conductivity of the electrolyte (Figure 3) [40, 42-44]. It was found that breakdown potential, final voltage and layer growth rate significantly increased with the sol concentration in the electrolyte [25, 40, 42, 45]. However, it was also reported that addition of such a sol to the electrolyte can delay the coating growth. Breakdown and final voltage were much lower when adding alumina sol to the electrolyte [24].

Summarizing, it can be stated that the effect of particle addition to the electrolyte via the sol route causes more influences on the electrical response of PEO process than the addition of powders. This is associated with the change of the composition, conductivity and viscosity of the electrolyte by the organic additives, which plays an important role in the electrical response of PEO process. Apart from that the influence depends very much on the base electrolyte, substrate, properties of the particles (type and size), power source as well as the electrical parameters applied during PEO treatment, so that no clear picture exists.

4 Uptake of particles and incorporation mechanisms of particles added into electrolytes

The mechanisms of particle uptake and incorporation into PEO coatings were discussed in a number of recent studies. The pores on the coating surface were considered as uptake paths for particles to enter into the coating, since the pores are normally filled with particles after PEO treatment [34, 46]. It was confirmed by Seyfoori et al. [47] that the accumulation of nanoparticles in the vicinity and inside the pores was higher than in the other zones. Arrabal et al. [31, 48] assumed that the particles were transferred to the interface between the inner and outer layer through short-circuit paths in the outer layer. A limited inward mass transfer of zirconia, up to a depth of 50% of the intermediate layer, was observed for three-layered coatings on Al by Matykina et al. [49] due to the appearance of "soft" sparking. The uptake of the particles was influenced and weakened by the reduced voltage under the "soft" sparking regime. Necula et al. [46] proposed that the mechanism of incorporation of Ag nanoparticles into the coating was a result of three main steps: delivery of particles to the sites of coating growth, entrapment of particles at the sites of coating growth and preservation of the embedded particles during layer growth. According to Lee et al. [34], electrophoretic deposition and mechanical mixing were the main factors leading to the incorporation of particles into the coatings on Mg alloy. It was also found that electrophoretic deposition played an important role in the incorporation of HA particles into PEO coatings on Ti [50-53]. Lu et al. [30, 54] have proposed that there are two steps, uptake and incorporation (Figure 4), to transfer particles from the electrolyte into the coating. The uptake of the negatively charged particles before the breakdown potential can be considered as an deposition/adsorption process in regions with enhanced anodic dissolution and strong re-deposition of conversion products [54, 55]. It was reported that the particle size has an

effect on the uptake process [30, 56]. Yeung et al. [56] proposed that nano-sized HA particles were more abundant and penetrated deeper in the coating compared to micro-sized particles, since large-sized particles were hardly to penetrate through the pores on the coating surface.

Particles can achieve either reactive or inert incorporation into the coating, depending on the substrate, applied electrical parameters, electrolyte composition and the properties of particles (size, melting temperature and chemical stability). Alteration of the electrical parameters can influence the incorporation mode [31, 55], which is mainly related to the change of energy of the discharges. Inert and reactive incorporation into the coating have been observed for ZrO_2 particles when using the same electrical conditions but various electrolytes [48]. Particles with smaller size [30, 54] and/or lower melting point [19, 57, 58] experience more easily reactive incorporation. Low melting point particles can also achieve inert incorporation into the coating when they have relatively high chemical stability [21]. In some cases solid state sintering can occur [59], resulting in fusion of particle boundaries with the surrounding oxide material. For other particles, e.g. ZrO_2, phase transformation was observed if they have different lattice modifications at different temperatures [48]. A more detailed summary about the observed reactions and coating compositions of PEO coatings with particle addition is given in the next paragraph.

5 Influence of particle addition on coating composition, microstructure and morphology

The composition of the PEO electrolyte is one key factor to determine the composition, microstructure and morphology of PEO coatings. Thus introduction of particles to the electrolyte will modify the coatings, such as phase composition, pore characteristic, thickness and

compactness of the layer. Detailed information of achieved compositions of PEO coatings as well as the substrate, electrolyte composition and incorporation mode of the particles is shown in Table 2 (Supplementary Material). A quick overview of the scope, size and incorporation mode of the particles for Mg, Al and Ti alloys is given in Figure 5 and the following sections discuss the particular aspects.

5.1 Mg and its alloys

5.1.1 Oxide particles

Various oxide particles have been used to modify PEO coatings on Mg and its alloys. In general, oxide particles with low melting point and small size can experience reactive incorporation more easily in comparison to high melting point and large-sized particles. For instance, clay particles (< 1200 °C) have achieved fully reactive incorporation into PEO coatings on AM50 Mg alloy [57, 58, 60]. In the presence of particles, the main fraction of the coating in the top and center region has been transformed from crystalline phase to amorphous phase (Figure 6), which had a composition close to commercial bio-glasses [57]. The ratio of amorphous to crystalline phases can be controlled by the KOH and Na_3PO_4 content in the electrolyte [60]. Also small-sized particles (SiO_2 nanoparticles) were reported to be melted, reacting with other components and resulting in higher fraction of amorphous phase in the coating. In contrast, the composition of coatings obtained in electrolytes with micro-sized SiO_2 particles was not affected greatly except the presence of inertly incorporated particles [30, 54]. Other oxide particles (ZrO_2, TiO_2 and Al_2O_3) with higher melting point were generally found to achieve inert incorporation [19, 23, 27,

34, 61-65] or partly reactive incorporation, resulting in formation of $Mg_2Zr_5O_{12}$, Mg_2TiO_4 and $MgAl_2O_4$ phases in the coatings [24, 26, 28, 29, 31, 48, 66-68].

The applied electrical and electrolyte conditions also determine the incorporation mode of the particles as well as the coating composition. For example, it was claimed that the incorporation of ZrO_2 particles into the coating can range from inert incorporation [19, 34] to partly reactive incorporation [31, 48, 68] under different treatment conditions. The $Mg_2Zr_5O_{12}$ reaction phase was only observed in the coating produced from phosphate electrolyte and not from silicate-based one [48]. However, the ZrO_2 particles achieved reactive incorporation in the same silicate electrolyte under AC instead of DC regime [31]. Commonly, the crystallinity of the layer increased with the energy input (current density/voltage) during PEO treatment [55, 58]. Furthermore the incorporation mode of the introduced particles can be considered as an indirect evidence for the plasma temperature during PEO treatment. It was found that the monoclinic zirconia transformed to tetragonal phase, indicating that the local temperature reached at least 1513 K [19, 48]. According to Lee et al. [19], it can be assumed that the temperature of the plasma was between 2116-2643 K, which are the melting temperatures of TiO_2 and ZrO_2 particles, since Mg_2TiO_4 was detected while ZrO_2 particles were inertly incorporated into the coating.

Introduction of particles has an effect on the microstructure and morphology of PEO coatings, e.g., pore characteristic, thickness and compactness of the layer. Addition of oxide particles to the electrolytes can reduce the number and/or size of the pores on the coating surface [23, 24, 30, 34, 38, 45, 57, 62, 65]. For instance, the surface of coatings with inertly incorporated titania from sol addition was much less porous (Figure 7) [23]. Normally sealing is more effective when adding

sols to the electrolyte and/or in the case of reactive incorporation. However, it was also claimed that the coating surface was not influenced too much [27, 61] or became more porous when oxide particles were added to the electrolytes [29]. The compactness and thickness of the layer can be altered or enhanced in the presence of oxide particles. It was reported that the outer layer of the coating became more compact and uniform [24, 27, 31, 45, 61, 68] compared with the coatings formed in particle free electrolytes. There is no clear trend for the influence of particles on the coating thickness. It was found that oxide particles were not effective to increase coating thickness, since the coatings generally demonstrated similar thickness [19, 27, 34] or even became thinner [30, 61] with addition of particles. Nevertheless, some reports claimed that the coatings were slightly thicker [28, 29, 62, 68] in the presence of particles. The change of the thickness of the particle-containing coatings is associated with the altered voltage/current evolution during PEO processing.

5.1.2 Non-oxide ceramic, organic and metallic particles

Non-oxide particles, e.g., inorganic (hydroxyapatite and Si_3N_4), organic (PTFE) and metallic particles (Ag), are generally inertly incorporated into the PEO layers [17, 21, 69-71]. In some cases, partly reactive incorporation can also be observed for HA and SiC particles [47, 72, 73] when the temperature and lifetime of the discharges are sufficient to melt/decompose the particles. For instance, the coatings produced from electrolyte containing HA particles were composed of hydroxyapatite and whitlockite (TCP) [47]. This discrepancy is probably ascribed to the different substrates, base electrolytes and electrical parameters utilized during PEO process. Inert incorporated particles are often reported to decrease the porosity of PEO coatings [21, 47, 69-71]. For example, the pores on the coating surface were smaller and more homogenous after

incorporation of PTFE particles [21]. The coating morphology has also been modified in the presence of particles. The cross section of the coating was reported to be denser, as through-going pores and defects were hardly detected in particle-containing coatings [21, 73]. In terms of coating thickness, thicker coatings were formed in SiC nanoparticles containing electrolyte under constant current regime [72]. The increment of the coating thickness depends on the applied current density. It is larger when using lower current density (Δ thickness=12 μm) in comparison to Δ thickness=5 μm at higher current density. It contrasts with coatings produced in PTFE and Si_3N_4 containing electrolytes, which were thinner compared with the coatings produced from particle-free electrolyte under constant voltage mode [21, 71]. This is probably caused by the different incorporation modes and applied electrical parameters.

Additionally, the substrate can serve as source of particles or fibers for PEO coatings if metal matrix composites are used. This review will only concern with the reinforcement similar in size and composition to the particles that are typically added to the electrolyte, for instance, SiC particles, usually used as reinforcement in PEO treatment of metal matrix composites [74, 75]. It was found that SiC particles were partly reactively incorporated into PEO coatings, as some particles were oxidized and then reacted with MgO to synthesize Mg_2SiO_4 phase (Figure 8) [76]. However, such a strong oxidation was not confirmed by Arrabal et al. [75, 77], which might be attributed to the large-sized embedded particles in the latter case. SiC particles were distributed throughout the layer and only a thin layer of reaction product, possibly silica, was formed at the particle/coating interface. The coating thickness was reduced by the particles, while the surface morphology was not significantly influenced in this case.

5.2 Al and its alloys

5.2.1 Oxide ceramic particles

Like for the coatings on Mg and its alloys, oxide particles can achieve reactive or inert incorporation into PEO coatings on Al-based substrates. It was reported that Al_2O_3 and TiO_2 particles can be reactively incorporated into PEO coatings [25, 59, 78], while inert incorporation also occurred for TiO_2 particles in some cases [79-81]. The reactively incorporated particles (Al_2O_3 and TiO_2) resulted in formation of mullite ($3Al_2O_3 \cdot 2SiO_2$), and Al_2TiO_5, Ti_2O_3 and TiO, respectively. Moreover, the coatings formed in Al_2O_3 containing electrolyte revealed an increased fraction of α-Al_2O_3 phase in the outer coating region [59]. Monoclinic zirconia particles were often transformed to higher temperature tetragonal or orthorhombic phases without formation of new compounds [32, 33, 49, 82, 83].

Different effects on the coating morphology were found for coatings with reactively incorporated oxide particles, which can be ascribed to the various types and sources of the particles used in the PEO treatment [25, 59, 78]. If titania is added as sol, the coating surface became rougher with more large-sized pores, and the coating thickness increased with increasing concentration of titania sol in the electrolyte [25, 78]. It was reported that the reactively incorporated Al_2O_3 particles did not change significantly the thickness and roughness of the coatings, and the coatings showed less porosity [59]. Inert incorporation of particles can decrease the coating porosity [79-81] and increase the coating thickness [32, 33, 49, 81]. Matykina et al. [32, 33, 49] have found that the distribution of the inertly incorporated ZrO_2 particles was different under DC and AC conditions. Zirconia was located at the coating surface and in the defects within the

coatings, and zirconia-rich regions with a cellular morphology was observed, indicating that melting of the coating occurred during DC treatment [33]. A limited inward mass transfer of zirconia, up to a depth of 50% of the intermediate layer, was found for coatings produced by the AC treatment [49].

5.2.2 Non-oxide and metallic particles

Generally, non-oxide particles, e.g., SiC, graphite, carbon nanotubes (CNTs) and Fe, were claimed to enter via inert incorporation into PEO coatings on Al and its alloys [20, 84-88]. It was found that the inertly incorporated CNTs contributed to the formation of more α-Al_2O_3 phase in the coating, leading to rougher surface with reduced coating thickness [85]. Coatings can also demonstrate lower roughness and similar thickness when the coating composition is not altered in the presence of particles [84, 86-88]. In addition, reactive incorporation of graphite particles into PEO coatings on 6061 Al alloy was observed by Ma et al. [89]. XRD results showed that the coatings consisted of η-Al_2O_3, graphite, Al_4C_3, Al_2OC and Al_4O_4C phases, in addition to α-Al_2O_3, γ-Al_2O_3, silica and aluminosilicate phases. The addition of these graphite particles had no effect on the coating thickness.

5.3 Ti and its alloys

5.3.1 Ceramic and metallic particles

It was found that particles (Al_2O_3, graphite, MoS_2, Ag and ceria) can be inertly incorporated [46, 90-93] into PEO coatings on Ti and its alloys or in a partly reactive mode (graphite, ZrO_2, HA, Cu, MnO_2/Mn_2O_3 and NiO) [22, 94-97]. For instance, Ti-C bonds were formed between TiO_2 and

graphite particles according to XPS measurements [96]. The reactive incorporation of MnO_2 and NiO into PEO coatings is mainly due to the addition of surfactants (sodium dodecyl sulfate and sodium oleate) to the electrolyte [22, 94]. Although the surfactants did not noticeably affect the content of Mn in the coatings but facilitated formation of Mn silicates, such as Mn_2SiO_4, $MnSiO_3$ and Mn_7SiO_{12}, whereas without surfactants only Mn_2SiO_4 was detected in the coatings [94]. However, it was also found that the surfactants can increase the nickel content from 3.2 to 14.3 at. % in the coating, and facilitate formation of Ni_2SiO_4 [22, 94]. The increased amount of Ni content was a result of higher final voltage registered for coatings produced from surfactant-containing electrolyte. In terms of coating morphology, incorporation of particles (graphite, Ag, MnO_2/Mn_2O_3 and NiO) can reduce the number of pores on the coating surface and enable the coating to be more uniform [22, 35, 91, 94, 96]. It was also claimed that the coating surface (size and shape of the pores) was not significantly influenced by the additional particles, although some particles can be observed on the coating surface [90, 95]. Incorporation of particles (e.g., MoS_2 and graphite) into PEO coatings has a negative effect on the layer thickness [90, 96]. For example, the coating thickness was reduced from 25 μm to 15 μm with addition of MoS_2 particles [90]. Jiang et al. [98] have produced PEO coatings with Ce^{3+} doped yttrium aluminium garnet (YAG: $Y_3Al_5O_{12}$) and found that the particles acted as nucleation sites for crystallization of titania, leading to reduced grain size from 20-21 nm to 13-14 nm.

5.3.2 In-situ formed particles

Many bioactive Ca-P-containing PEO coatings were formed in electrolytes containing soluble Ca and P salts, such as calcium acetate and sodium ortho- or hydrogen phosphates [99-102]. However, in reality such electrolytes present suspensions, since the reaction between the above

electrolyte components leads to the precipitation of calcium phosphates or hydrogen phosphates. Therefore they can be considered as particle-containing electrolytes. The phase composition of the coatings produced in suspensions of calcium phosphates strongly depends on the PEO regime. For instance, Matykina et al. [99] and Whiteside et al. [100] both using constant current DC regime obtained coatings containing anatase and rutile, where Ca and P were present as an amorphous phase. Constant voltage AC [101, 102] and bipolar [103] regimes produced crystalline Ca- and P-containing phases, such as apatite, hydroxyapatite and calcium titanate (Figure 9). Formation of crystalline phases in constant voltage regime must be apparently associated with high peak currents (and, hence, temperatures inside the discharge channels) achieved at the beginning of the positive pulse.

6 Influence of particle addition on coating properties

The demand of modern technological society for light structural materials (Mg, Al and Ti) emphasizes a combination of good corrosion resistance with wear resistance and functionalized surfaces. The applications can range from structural and transport components to bioengineering. Regardless of the final application, improved tailored surfaces are required to prolong service life and reduce long-term costs. Additional phases, thicker or denser layer can be used to tune better and/or new properties for PEO coatings (Table 3 and Table 4, Supplementary Material), for instance, better corrosion performance (ZrO_2, TiO_2 and CeO_2), higher hardness (Al_2O_3 and SiC), lubricity (PTFE, MoS_2 and graphite), bioactivity and biocompatibility (HA and calcium phosphates), ferromagnetic properties (Co and Fe/Fe_2O_3), antibacterial (Ag and Cu) and catalytic activities (TiO_2, ZrO_2, Fe_2O_3, Ni/NiO and MnO_2/Mn_2O_3).

6.1 Mg and its alloys

6.1.1 Mechanical and tribological properties

Due to the high porosity and limited range of phase compositions, PEO coatings on Mg and its alloys are unable to provide long-term wear protection. In order to overcome the drawbacks, either the porosity of the outer layer is suppressed or new stable phases are formed in the coating with the aid of particles. Incorporation of hard particles (inert incorporation [30, 62, 77]) or formation of new phases with high hardness (reactive incorporation [29, 30]) can increase wear resistance. For the PEO coated Mg alloy AZ31, the hardness increased from 130 HV to 358 HV due to inertly incorporated Al_2O_3 nanoparticles. Consequently, the wear track (Figure 10) of coating with particle addition was much narrower and shallower in contrast to that of particle-free coating [62]. The hardness of PEO coatings on AZ91D Mg alloy was also increased by reactive incorporation of Al_2O_3 nanoparticles [29]. Figure 11 shows that the coating hardness increased from ~150 HV to ~375 HV with the increase of particle concentration in the electrolyte, which was related to the significant increase of $MgAl_2O_4$ phase in the layer. PEO coatings can also demonstrate higher hardness and better wear performance due to the denser and/or thicker layer after incorporation of particles (SiC and TiO_2) [63, 65, 72, 104]. Furthermore, solid lubricant particles (PTFE) were introduced to PEO coatings aiming to reduce the friction coefficient [21]. As a result, the friction coefficient of coatings with PTFE was stable and much lower (below 0.2) in comparison to that of coatings free of particles (0.5-0.7), preventing wear of the surface.

6.1.2 Corrosion performance

Regarding the corrosion behavior, different particles (ZrO_2, TiO_2, and CeO_2) have been utilized to improve the corrosion performance of PEO coatings on Mg and its alloys (Table 4, Supplementary Material), but controversial results have also been found. Enhanced corrosion properties are mainly caused by newly formed stable phases (reactive incorporation of particles [28, 68]) or by the inertly incorporated particles [23, 27, 34, 61, 65] which have high chemical stability. For instance, the corrosion resistance of PEO coatings can be greatly improved by addition of ZrO_2 particles [34, 68]. After inert incorporation of ZrO_2 particles (200-400 nm), the corrosion current density (i_{corr}) of the coated Mg alloy was reduced from 7.27×10^{-7} A/cm^2 to 7.03×10^{-8} A/cm^2 with respective increase of polarization resistance and shift of the corrosion potential towards more positive values. Salt spray test demonstrated that the incorporation of ZrO_2 particles efficiently minimizes the incidence of pitting corrosion on PEO coated substrates [34]. Reactive incorporation of ZrO_2 obtained via sol route can also improve the corrosion performance of PEO coatings [68]. The corrosion current density was reduced by about two times and the corrosion potential significantly shifted to positive direction (from -1.50 V vs SCE to -1.22 V vs SCE). In some cases PEO coatings become denser or thicker thus demonstrating better barrier properties after inert incorporation [21, 24, 40, 42, 62] or reactive incorporation [45] of particles. The improvement of the corrosion resistance is often attributed to the denser and thicker layer after particle addition. However coatings can also be more porous when the particle concentration in the electrolyte is beyond certain level, which is detrimental to the corrosion performance of PEO coated Mg [61]. Inertly incorporated particles can be considered as containers to load inhibitors to achieve self-healing functionality for PEO coatings. Sun et al. [38]

used halloysite nanotubes as nanocontainers to load inhibitors (benzotriazole). The inhibitor containing PEO coatings confer active corrosion protection responding to the pH change triggered by the corrosion process.

HA particles were used not only to improve the corrosion performance but also to provide apatite formation ability for PEO coatings on Mg alloys [47, 69, 70, 73]. Figure 12 shows the Nyquist and Bode plots of the coatings with and without particle addition. The resistance of the outer layer has increased by 3 times as a result of particle incorporation. Moreover introduction of HA particles endow the layer with superior apatite forming ability. The amount of apatite (Figure 13) formed on the coating surface after 3 days of immersion was higher than that of blank PEO coating [47].

Although the abovementioned studies proved that particle addition can provide better corrosion resistance for PEO coatings, the improved properties show limitations depending on the amount of particles used in the electrolyte. The long-term performance of the coatings is also an issue. In some cases additional particles are not effective or even deteriorating the corrosion protection performance of the coatings during long-term corrosion tests [30, 60, 64, 71]. According to Lu et al. [30], addition of SiO_2 particles (12 nm and 1-5 μm) can improve the short-term resistance but deteriorate the long-term resistance of PEO coatings, since the coatings in the presence of particles demonstrated a faster degradation rate, reaching similar value as the coatings free of particles. The smaller the particle size was, the more variations in corrosion properties were observed. Wang et al. [64] demonstrated that coatings produced from electrolytes containing 5 and 10 vol. % titania sol showed worse corrosion resistance than that of the unmodified coatings

after relatively long-term immersion in SBF (Figure 14), which was attributed to the increasing amount of amorphous material by the incorporation of TiO_2.

6.1.3 Other properties

The incorporation of particles allows creating surfaces with different functionalities such as hydrophobicity or enhanced photocatalytic properties. PEO coated AM60B Mg alloy was reported to show hydrophobicity after incorporation of polytetrafluoroethylene (PTFE) hydrophobic particles [21, 105]. The contact angle of the coatings has been increased from 50°-55° to 92°-101° after inert incorporation of PTFE particles [21]. Based on well-known photocatalytic properties [106], TiO_2 particles were introduced to PEO coatings to provide this additional functionality for Mg alloy surface. It was found that PEO coatings with TiO_2 nanoparticle additions on AZ91D Mg alloy showed good photocatalytic performance (Figure 15), as the inertly incorporated TiO_2 particles greatly accelerated the decomposition rate of methylthionine blue solution [28]. Furthermore, additional particles are favorable to colorize PEO coatings. Introduction of TiO_2 particles to the electrolyte produced blue PEO coatings [28, 67] and the white-grey coatings became darker after incorporation of Ag nanoparticles [17].

6.2 Al and its alloys

6.2.1 Mechanical and tribological properties

Introduction of particles to PEO coatings can promote α-Al_2O_3 formation or coating densification resulting in enhanced tribological properties of Al and its alloys. The coating hardness can be increased via addition of high-hardness particles [59]. Figure 16 shows that the addition of

alumina particles did not modify the hardness of the inner layer but increased that of the outer layer due to increased proportion of α-Al_2O_3 phase formation. The wear performance of the coating produced in the electrolyte with 10 g/L particle addition was even better than that of a conventional hard chrome coating. Addition of particles (ZrO_2, TiO_2 and Fe) facilitate formation of thicker [25] or densified layer [80, 83, 84] which can also provide higher hardness for PEO coatings. The addition of ZrO_2 particles increased the hardness of PEO coatings on ADC12 Al alloy from 500 HV to 800 HV, which was attributed to the more compact and uniform coating after inert incorporation of ZrO_2 particles [83]. The ZrO_2-containing coatings showed improved tribological behavior with more stable and lower friction coefficient (reduced from ~0.6 to ~0.2). Particles with lubrication properties (graphite and carbon nanotubes) were introduced to electrolyte to produce PEO coatings on Al and its alloys [85, 87, 89]. PEO coatings with partly reactively incorporated graphite particles showed relatively low friction coefficient (0.12) when sliding against a tungsten carbide/cobalt ball under a load of 5N. In contrast, the friction coefficient of the coatings without particle addition was 0.6 [89].

6.2.2 Corrosion behavior

Particles have been added to PEO coatings to improve the corrosion performance of Al and its alloys [20, 37, 79]. Multi-walled carbon nanotubes (MWCNTs) were added to PEO coatings on 7075 Al alloy by Lee et al. [20]. The corrosion current density of the layer decreased from 4.6×10^{-9} A/cm^2 to 8.3×10^{-10} A/cm^2 in the presence of particles in 3.5% NaCl solution. Bahramian et al. [79] studied the effect of TiO_2 particles on the corrosion behavior of PEO treated 7075 Al alloy in 1 M H_2SO_4 solution. Electrochemical measurements showed that the corrosion current density of the PEO coatings decreased from 40±7 μA/cm^2 to 15±1 μA/cm^2 after

inert incorporation of TiO_2 particles, but the corrosion potential was not considerably changed. It was claimed that the improved coating property was attributed to the lower coating porosity with TiO_2 addition.

6.3 Ti and its alloys

6.3.1 Mechanical and tribological properties

Solid lubricant particles (graphite and MoS_2) have been added to electrolyte to reduce the friction coefficient of PEO coatings [90, 96]. Although the coating was thinner, the friction coefficient of the coating was decreased from 0.6-0.8 to 0.15 after inert incorporation of graphite particles, leading to a reduced volume of the wear track (Figure 17). The wear rate of the uncoated alloy, coating with and without particle addition was measured to be 5.2×10^{-5} $mm^3/N\,m$, 8.6×10^{-6} $mm^3/N\,m$ and 1.7×10^{-5} $mm^3/N\,m$, respectively [96].

6.3.2 Catalytic activities

Although the PEO coated Ti substrates has catalytic activities, a limitation of TiO_2 is a fast recombination of photogenerated electron-hole pairs, which can be overcome by doping of TiO_2 with other semiconductor materials, such as ZrO_2. Recently, several studies of photocatalysts based on ZrO_2-containing PEO coatings on Ti alloys have been carried out [107, 108]. For instance, Luo et al. [108] produced ZrO_2/TiO_2 composite photocatalytic films in colloidal $Zr(OH)_4$ particle-loaded electrolyte. The K_2ZrF_6 additive was used in alkaline electrolyte to precipitate $Zr(OH)_4$ according to the reaction: $K_2ZrF_6 + 4NaOH \rightarrow Zr(OH)_4\downarrow + 2KF + 4NaF$. The photocatalytic activity evaluation was based on degradation rate of rhodamine B solution under

ultraviolet irradiation. The degradation rate was reported to be about 3 times higher for a ZrO_2/TiO_2 composite coating compared with pure TiO_2 coating, 0.0442 and 0.0186 h^{-1}, respectively. Another option is to introduce YAG: Ce^{3+} to PEO coatings on Ti6Al4V alloy [98]. The composite coatings exhibited much larger specific surface area, higher absorption of visible light and higher photocurrent (Figure 18) compared to that of the particle-free coatings. Thus the decomposition of methyl blue increased from 50 % to 70 % after the same exposure time of 3 hours. Incorporation of transition metals, such as Fe cations into TiO_2 enables the excitation of the latter in the UV but also in the visible light region, thus enhancing the efficiency of the photocatalysis under sunlight conditions. Soejima et al. [109] investigated the photocatalytic activity of Fe^{3+}-doped anatase-rutile TiO_2 films on pure Ti with respect to decomposition of acetaldehyde as a function of the irradiation time and the concentration of Fe_2O_3 in the electrolyte. The optimum Fe content (x=3 g/L of added Fe_2O_3) showed maximum of both UV and visible light photocatalytic activity compared with that of pure TiO_2 films. Another possible application is the oxidation of CO to CO_2. Vasil'eva et al. [94] have studied the catalytic activity of Mn-TiO_2 catalysts with respect to oxidation of CO into CO_2 at 500 °C. Using a gas analyzer and a gas flow device showed that conversion of CO into CO_2 is low (11%) but increases up to 20 % and 28 % for the coatings obtained in the electrolytes with sodium dodecyl sulfate and sodium oleate, respectively. Incorporation of NiO into PEO coatings on c.p. Ti is even more effective. The Ni-containing TiO_2 coatings are demonstrated to be effective catalysts, increasing the CO conversion up to 80 % at 500 ºC [22, 94].

6.3.3 Ferromagnetic property

Rudnev et al. [110] have produced ferromagnetic PEO coatings by addition of particles. A $Na_3PO_4/Na_2B_4O_7/Na_2WO_4$ based electrolyte was used containing, variably, iron oxalate, copper acetate or nickel (II) salt and $Fe_2(C_2O_4)_3$, the latter being practically insoluble. The coercive force of the coatings examined at 300 K and 10 K reached maximum values of 124 Oe and 380 Oe, respectively, which is associated with the presence of conglomerates of ~50 nm crystallites, containing metallic Fe (predominantly), Ti, W and their oxides located mostly in the outer part of the coating. Gnedenkov et al. [111] studied the magnetic properties of PEO coatings modified by nanoparticles of cobalt (33-106 nm) on titanium. The magnetic properties (magnetization and coercivity) of the coatings (514 Oe at room temperature and 1024 Oe at 2 K) were ascribed to the nanosize effects of particles embedded in the coating. The particles consisted of a ferromagnetic Co core and an antiferromagnetic CoO/Co_2O_3 shell.

6.3.4 Bioactivity, biocompatibility and antibacterial activities

Bai et al. [112] have compared the proliferation and alkaline phosphatize activity of mouse osteoblast cell cultured on coatings with and without hydroxyapatite nanoparticles. The HA-containing coatings showed positive correlation of the apatite-forming ability during immersion in SBF solution. In addition, the HA-containing coatings exhibited greater cell proliferation and ALP levels (i.e. greater maturation of the extracellular matrix) than the coatings without particles, which is beneficial for osseointegration [113]. Kim et al. [50] corroborates the ALP-related findings for similarly obtained HA-PEO coatings. Lee et al. [53] have demonstrated that the osteoblast cell viability increases with the HA content in the electrolyte (and consequently in the

coating). The size of the HA particles appears to have a considerable effect on their incorporation and distribution within the coatings and subsequent bioactivity of the latter as recently demonstrated by Yeung et al. [56], who studied PEO of Ti-6Al-4V alloy in the electrolytes with added micro-size (2.5 μm) and nano-size HA particles. Specifically, the nano-size particles were found to be more abundant and penetrate deeper in the coating without altering the surface pore morphology of the coating. This is believed to be related to a greater negative charge and mobility of nano-sized HA particles compared with micro-sized HA. As a result, the coatings with nano-HA particles exhibited an enhanced biomimetic precipitation of HA during immersion in SBF and greater ALP activity of mouse osteoblast cells compared to those with micro-size HA particles.

The in-vitro biological responses of Ti6Al4V and Ti6Al7Nb alloys with ~10 μm-thick PEO coatings produced in calcium acetate/sodium orthophosphate electrolyte was evaluated by Cimenoglu et al. [103]. Both coatings comprised anatase and rutile. Additionally, hydroxyapatite and calcium titanate were present in the coatings formed on Ti6Al4V and Ti6Al7Nb alloy, respectively. Both coatings exhibited similar hydroxyapatite inducing ability during immersion in SBF. The human osteosarcoma (SAOS-2) cell proliferation was greater on the coated Ti6Al4V alloy than on the Ti6Al7Nb alloy.

The influence of different Ca/P atomic ratios generated in calcium phosphate-based suspensions on the bioactivity of PEO coatings on pure Ti was studied by Mohedano et al. [101]. They observed a faster mouse osteoblast cell proliferation rate on the coating with Ca and P in the amorphous phase and Ca/P ratio of 4.0 than on the one with $Ca_3(PO_4)_2$ and Ca/P ratio of 1.7. The authors concluded that high Ca/P ratio is more important to accelerate the initial cell response

than a high percentage of Ca and P in the coating material, because the chemical activity of doping Ca ions is higher than that of the ions bound into crystalline compounds. Whiteside et al. [100] investigated bioactivity of ~8-15 μm-thick Ca- and P-containing coatings produced on pure Ti under DC conditions in calcium phosphate suspension electrolytes. The Ca/P ratio in the coating varied from 0.14 to 0.46 and (Ca+P)/Ti ratio from 0.52 to 0.90. Despite these relatively low values and the absence of crystalline Ca-P phases in the oxide material, the proliferation rates of primary human osteoblasts cells on the coatings were up to ~37% faster than those for uncoated reference materials. Additionally, the amount of collagen generated by the cells on the coatings was up to ~2.4 times greater than for the reference substrates. Not only Ca and P containing particles and phases do have a positive effect on the bioactivity.

Shin et al. [114-116] have investigated the bioactivity of PEO coatings with tetragonal zirconia (t-ZrO_2) particles on pure titanium. The particles have facilitated the nucleation and growth of biomimetic apatite on the coating surface during immersion in SBF. Also, the growth and proliferation rates of the mouse osteoblasts were higher on the coating with t-ZrO_2 particles compared to that for the particle-free layers. Although the particles did not affect the size and fraction of the micropores, they resulted in a surface with higher roughness, which was observed to facilitate the extension and interlocking of the filopodia.

Due to the good antibacterial activity of Ag [117], PEO coatings with unreacted Ag particles demonstrated a well-defined antimicrobial effect. Bactericidal coatings were successfully produced on a titanium medical alloy using Ag nanoparticles containing PEO electrolyte [35]. Quantitative cultures after 24 h of incubation clearly showed the bactericidal activity of the TiO_2-Ag composite coatings (no colonies present on the blood agar plates at any dilution). MRSA

inocula was completely killed within 24 h, even in the presence of 50% human serum, while ground and oxidized titanium in the absence of Ag nanoparticles showed a 1000-fold increase in bacteria CFU. Teker et al. [118] have demonstrated antibacterial activity of Ag-containing PEO coatings on Grade 4 Ti with respect to *Escherichia coli* (*E. coli*) and *Staphylococcus aureus* (*S. aureus*). The coatings were produced in calcium acetate/disodum hydrogen phosphate suspension electrolyte, but the source of Ag was introduced in the form of soluble silver acetate. The resultant coatings contained hydroxyapatite, $CaTiO_3$ and 4.6 wt. % of Ag and have inhibited the numbers of *E. coli* and *S. aureus* inoculated up to > 99.9% and 99.8%, respectively, after a 24 h incubation period (Figure 19). Ag-free PEO coating also showed some bactericidal effect, eliminating 58.3% and 48.7%, *E. coli* and *S. aureus*, respectively, which was attributed to the photocatalytic activity of TiO_2: the reactive oxygen species and/or OH^- radicals are believed to attack the bacteria membrane. Another metal which is known for its antibacterial activity is Cu. The antibacterial effect of Cu nanoparticles in PEO coatings on c.p. Ti with respect to *E. coli* and *S. aureus* was investigated by Yao et al. [95]. Cu nanoparticles (up to 2.5 wt. %) were found on the coatings surface and embedded in the coating. The XPS examination revealed that Cu in the coatings mainly existed in the Cu^{2+} state. The qualitative fluorescent examination of the bacteria inoculated materials showed that Cu-doped coating eliminated most of the two species of bacteria, although little information exists on the particulars of antibacterial mechanism of Cu.

7 Conclusions and outlook

In summary, introduction of particles is an effective approach to modify and optimize the composition, microstructure, morphology and properties of PEO coatings. The composition of the coating is associated with the incorporation mode of the particles. The incorporation mode of

the particles is mainly related to the possibility of chemical reaction between them and the main metallic oxides (MgO, Al_2O_3 and TiO_2) generated by the substrate/electrolyte combinations. Hence oxide particles can more easily achieve reactive incorporation into the coating in comparison to organic, metallic, carbide and nitride particles. The electrical parameters applied during PEO treatment play a vital role in the uptake and incorporation mode of the particles as well. For some particles the mode of incorporation can be changed and controlled by the electrolyte parameters. In some cases, inert incorporation of particles seems to be more desirable, since they can enable PEO coatings with new functionalities due to their specific properties. In other cases reactive incorporation might be beneficial if the structure can be fully altered offering new properties. Sealing is more effective in the case of a reactive incorporation, while introduction of particles cannot fully seal the porosity of PEO coatings. The influence of particle addition on the coating thickness/growth rate is non-significant in comparison to the coating composition, which is mainly related to the evolution of voltage and current density during PEO process.

The addition of particles has significant effects on the properties of PEO coatings and provides multifunctionality for certain potential applications. Although particles can be used as additive to improve the corrosion performance of PEO coatings for short-term, the intrinsic porosity of the layer remains an issue for industrial application. Hence duplex/post-treatment is required to achieve long-term corrosion protection. In terms of wear and bio-application, addition of particles to PEO layers is of great potential. The layers in the presence of particles can demonstrate superior hardness and lubricating property providing desirable wear protection for the substrate. It is likely that particles loaded PEO coatings can exhibit biological properties, such as surface

bioactivity, antibacterial activities, apatite forming ability and controllable degradation ability. Incorporation of ferromagnetic particles or insoluble iron salt particles confers magnetic properties to the coatings for use in microelectronic applications, for instance in microtransformers and magnetic switchers.

In spite of the large list of possible applications, it must be stated that none of the coatings formed in electrolytes with particle additions is used commercially in an industrial application up to now, which might be related to the fact that keeping the particles uniformly dispersed is a challenge especially in large industrial treatment baths. Research of effective surfactants stabilizing dispersions is needed for the future. Repeated use of the electrolyte may weaken it due to the consumption of the particles. However, no quantitative information appears to be available regarding the effective ampere-hours of the electrolyte, particle consumption rate, degree of the deterioration of the coating quality, frequency of the electrolyte correction and associated costs etc. Therefore future work should be dedicated to systematic applied studies required for up-scaling of the particle-based PEO processes. There are some concerns in using this approach. Use of small-sized particles can cause health problems, such as respiratory disease, during preparation and disposal of the electrolytes. Although there are remaining issues and challenges, new research field can be opened regarding the introduction of particles to PEO coatings. For instance, particles can be regarded as perspective containers for loading corrosion inhibitors and be subsequently incorporated into the coating to confer self-sealing functionality during corrosion process. The metallic surface can be tuned and functionalized by PEO technique via addition of particles for a wider range of applications.

Acknowledgements

X. Lu thanks China Scholarship Council (201207090010) for the award of fellowship and funding. M. Mohedano is grateful to the Alexander von Humboldt Foundation (7000273793), Germany, for the award of AvH research fellowship and financial assistance. The authors are grateful to MINECO/FEDER (Spain, Project MAT2015-66334-C3-3-R).

References

[1] A.L. Yerokhin, X. Nie, A. Leyland, A. Matthews, S.J. Dowey, Plasma electrolysis for surface engineering, Surf. Coat. Technol., 122 (1999) 73-93.

[2] J.A. Curran, T.W. Clyne, Thermo-physical properties of plasma electrolytic oxide coatings on aluminium, Surf. Coat. Technol., 199 (2005) 168-176.

[3] R. Arrabal, E. Matykina, T. Hashimoto, P. Skeldon, G.E. Thompson, Characterization of AC PEO coatings on magnesium alloys, Surf. Coat. Technol., 203 (2009) 2207-2220.

[4] Y. Song, K. Dong, D. Shan, E.-H. Han, Investigation of a novel self-sealing pore micro-arc oxidation film on AM60 magnesium alloy, J. Magnesium Alloy., 1 (2013) 82-87.

[5] S. Yagi, K. Kuwabara, Y. Fukuta, K. Kubota, E. Matsubara, Formation of self-repairing anodized film on ACM522 magnesium alloy by plasma electrolytic oxidation, Corros. Sci., 73 (2013) 188-195.

[6] E. Matykina, A. Berkani, P. Skeldon, G.E. Thompson, Real-time imaging of coating growth during plasma electrolytic oxidation of titanium, Electrochim. Acta, 53 (2007) 1987-1994.

[7] R.O. Hussein, D.O. Northwood, X. Nie, The effect of processing parameters and substrate composition on the corrosion resistance of plasma electrolytic oxidation (PEO) coated magnesium alloys, Surf. Coat. Technol., 237 (2013) 357-368.

[8] C.E. Barchiche, E. Rocca, C. Juers, J. Hazan, J. Steinmetz, Corrosion resistance of plasma-anodized AZ91D magnesium alloy by electrochemical methods, Electrochim. Acta, 53 (2007) 417-425.

[9] P. Bala Srinivasan, J. Liang, C. Blawert, M. Störmer, W. Dietzel, Effect of current density on the microstructure and corrosion behaviour of plasma electrolytic oxidation treated AM50 magnesium alloy, Appl. Surf. Sci., 255 (2009) 4212-4218.

[10] R.O. Hussein, P. Zhang, X. Nie, Y. Xia, D.O. Northwood, The effect of current mode and discharge type on the corrosion resistance of plasma electrolytic oxidation (PEO) coated magnesium alloy AJ62, Surf. Coat. Technol., 206 (2011) 1990-1997.

[11] S. Aliasghari, P. Skeldon, G.E. Thompson, Plasma electrolytic oxidation of titanium in a phosphate/silicate electrolyte and tribological performance of the coatings, Appl. Surf. Sci., 316 (2014) 463-476.

[12] V. Dehnavi, B.L. Luan, X.Y. Liu, D.W. Shoesmith, S. Rohani, Correlation between plasma electrolytic oxidation treatment stages and coating microstructure on aluminum under unipolar pulsed DC mode, Surf. Coat. Technol., 269 (2015) 91-99.

[13] G. Lv, W. Gu, H. Chen, W. Feng, M.L. Khosa, L. Li, E. Niu, G. Zhang, S.-Z. Yang, Characteristic of ceramic coatings on aluminum by plasma electrolytic oxidation in silicate and phosphate electrolyte, Appl. Surf. Sci., 253 (2006) 2947-2952.

[14] C. Blawert, V. Heitmann, W. Dietzel, H.M. Nykyforchyn, M.D. Klapkiv, Influence of electrolyte on corrosion properties of plasma electrolytic conversion coated magnesium alloys, Surf. Coat. Tech., 201 (2007) 8709-8714.

[15] A. Ghasemi, V.S. Raja, C. Blawert, W. Dietzel, K.U. Kainer, The role of anions in the formation and corrosion resistance of the plasma electrolytic oxidation coatings, Surf. Coat. Technol., 204 (2010) 1469-1478.

[16] M. Shokouhfar, C. Dehghanian, M. Montazeri, A. Baradaran, Preparation of ceramic coating on Ti substrate by plasma electrolytic oxidation in different electrolytes and evaluation of its corrosion resistance: Part II, Appl. Surf. Sci., 258 (2012) 2416-2423.

[17] B.S. Necula, L.E. Fratila-Apachitei, A. Berkani, I. Apachitei, J. Duszczyk, Enrichment of anodic MgO layers with Ag nanoparticles for biomedical applications, J. Mater. Sci. Mater. Med., 20 (2009) 339-345.

[18] D. Hanaor, M. Michelazzi, C. Leonelli, C.C. Sorrell, The effects of carboxylic acids on the aqueous dispersion and electrophoretic deposition of ZrO2, J. Eur. Ceram. Soc., 32 (2012) 235-244.

[19] K.M. Lee, B.U. Lee, S.I. Yoon, E.S. Lee, B. Yoo, D.H. Shin, Evaluation of plasma temperature during plasma oxidation processing of AZ91 Mg alloy through analysis of the melting behavior of incorporated particles, Electrochim. Acta, 67 (2012) 6-11.

[20] K.M. Lee, Y.G. Ko, D.H. Shin, Incorporation of multi-walled carbon nanotubes into the oxide layer on a 7075 Al alloy coated by plasma electrolytic oxidation: Coating structure and corrosion properties, Curr. Appl. Phys., 11 (2011) S55-S59.

[21] J. Guo, L. Wang, S.C. Wang, J. Liang, Q. Xue, F. Yan, Preparation and performance of a novel multifunctional plasma electrolytic oxidation composite coating formed on magnesium alloy, J. Mater. Sci., 44 (2009) 1998-2006.

[22] M.S. Vasilyeva, V.S. Rudnev, I.A. Korotenko, P.M. Nedozorov, Producing and studying oxide coatings containing manganese and nickel compounds on titanium from electrolyte suspensions, Prot. Met. Phys. Chem. Surf., 48 (2012) 106-115.

[23] J. Liang, L. Hu, J. Hao, Preparation and characterization of oxide films containing crystalline TiO2 on magnesium alloy by plasma electrolytic oxidation, Electrochim. Acta, 52 (2007) 4836-4840.

[24] M. Laleh, A.S. Rouhaghdam, T. Shahrabi, A. Shanghi, Effect of alumina sol addition to micro-arc oxidation electrolyte on the properties of MAO coatings formed on magnesium alloy AZ91D, J. Alloy. Compd., 496 (2010) 548-552.

[25] M. Tang, W. Li, H. Liu, L. Zhu, Influence of titania sol in the electrolyte on characteristics of the microarc oxidation coating formed on 2A70 aluminum alloy, Surf. Coat. Technol., 205 (2011) 4135-4140.

[26] X. Li, B.L. Luan, Discovery of Al2O3 particles incorporation mechanism in plasma electrolytic oxidation of AM60B magnesium alloy, Mater. Lett., 86 (2012) 88-91.

[27] T.S. Lim, H.S. Ryu, S.-H. Hong, Electrochemical corrosion properties of CeO2-containing coatings on AZ31 magnesium alloys prepared by plasma electrolytic oxidation, Corros. Sci., 62 (2012) 104-111.

[28] W. Li, M. Tang, L. Zhu, H. Liu, Formation of microarc oxidation coatings on magnesium alloy with photocatalytic performance, Appl. Surf. Sci., 258 (2012) 10017-10021.

[29] Y. Wang, D. Wei, J. Yu, S. Di, Effects of Al2O3 Nano-additive on Performance of Micro-arc Oxidation Coatings Formed on AZ91D Mg Alloy, J. Mater. Sci. Technol., 30 (2014) 984-990.

[30] X. Lu, C. Blawert, Y. Huang, H. Ovri, M.L. Zheludkevich, K.U. Kainer, Plasma electrolytic oxidation coatings on Mg alloy with addition of SiO2 particles, Electrochim. Acta, 187 (2016) 20-33.

[31] R. Arrabal, E. Matykina, F. Viejo, P. Skeldon, G.E. Thompson, M.C. Merino, AC plasma electrolytic oxidation of magnesium with zirconia nanoparticles, Appl. Surf. Sci., 254 (2008) 6937-6942.

[32] E. Matykina, R. Arrabal, P. Skeldon, G.E. Thompson, Incorporation of zirconia nanoparticles into coatings formed on aluminium by AC plasma electrolytic oxidation, J. Appl. Electrochem., 38 (2008) 1375-1383.

[33] E. Matykina, R. Arrabal, F. Monfort, P. Skeldon, G.E. Thompson, Incorporation of zirconia into coatings formed by DC plasma electrolytic oxidation of aluminium in nanoparticle suspensions, Appl. Surf. Sci., 255 (2008) 2830-2839.

[34] K.M. Lee, K.R. Shin, S. Namgung, B. Yoo, D.H. Shin, Electrochemical response of ZrO2-incorporated oxide layer on AZ91 Mg alloy processed by plasma electrolytic oxidation, Surf. Coat. Technol., 205 (2011) 3779-3784.

[35] B.S. Necula, L.E. Fratila-Apachitei, S.A.J. Zaat, I. Apachitei, J. Duszczyk, In vitro antibacterial activity of porous TiO2–Ag composite layers against methicillin-resistant Staphylococcus aureus, Acta Biomater., 5 (2009) 3573-3580.

[36] H. Nasiri Vatan, R. Ebrahimi-kahrizsangi, M. Kasiri-asgarani, Structural, tribological and electrochemical behavior of SiC nanocomposite oxide coatings fabricated by plasma electrolytic oxidation (PEO) on AZ31 magnesium alloy, J. Alloy. Compd., 683 (2016) 241-255.

[37] D. Kim, D. Sung, J. Lee, Y. Kim, W. Chung, Composite plasma electrolytic oxidation to improve the thermal radiation performance and corrosion resistance on an Al substrate, Appl. Surf. Sci., 357, Part B (2015) 1396-1402.

[38] M. Sun, A. Yerokhin, M.Y. Bychkova, D.V. Shtansky, E.A. Levashov, A. Matthews, Self-healing plasma electrolytic oxidation coatings doped with benzotriazole loaded halloysite nanotubes on AM50 magnesium alloy, Corros. Sci., in press.

[39] M. Shokouhfar, S.R. Allahkaram, Formation mechanism and surface characterization of ceramic composite coatings on pure titanium prepared by micro-arc oxidation in electrolytes containing nanoparticles, Surf. Coat. Technol., 291 (2016) 396-405.

[40] W.P. Li, L.Q. Zhu, Y.H. Li, Electrochemical oxidation characteristic of AZ91D magnesium alloy under the action of silica sol, Surf. Coat. Tech., 201 (2006) 1085-1092.

[41] G. Yan, W. Guixiang, D. Guojun, G. Fan, Z. Lili, Z. Milin, Corrosion resistance of anodized AZ31 Mg alloy in borate solution containing titania sol, J. Alloy. Compd., 463 (2008) 458-461.

[42] W.P. Li, L.Q. Zhu, H.C. Liu, Preparation of hydrophobic anodic film on AZ91D magnesium alloy in silicate solution containing silica sol, Surf. Coat. Tech., 201 (2006) 2573-2577.

[43] L.Q. Zhu, Y.H. Li, W.P. Li, Influence of silica sol particle behavior on the magnesium anodizing process with different anions addition, Surf. Coat. Tech., 202 (2008) 5853-5857.

[44] W. Li, L. Zhu, H. Liu, Effects of silicate concentration on anodic films formed on AZ91D magnesium alloy in solution containing silica sol, Surf. Coat. Technol., 201 (2006) 2505-2511.

[45] J. Liu, Y. Lu, X. Jing, Y. Yuan, M. Zhang, Characterization of plasma electrolytic oxidation coatings formed on Mg–Li alloy in an alkaline silicate electrolyte containing silica sol, Mater. Corros., 60 (2009) 865-870.

[46] B.S. Necula, I. Apachitei, F.D. Tichelaar, L.E. Fratila-Apachitei, J. Duszczyk, An electron microscopical study on the growth of TiO2–Ag antibacterial coatings on Ti6Al7Nb biomedical alloy, Acta Biomater., 7 (2011) 2751-2757.

[47] A. Seyfoori, S. Mirdamadi, Z.S. Seyedraoufi, A. Khavandi, M. Aliofkhazraei, Synthesis of biphasic calcium phosphate containing nanostructured films by micro arc oxidation on magnesium alloy, Mater. Chem. Phys., 142 (2013) 87-94.

[48] R. Arrabal, E. Matykina, P. Skeldon, G.E. Thompson, Incorporation of zirconia particles into coatings formed on magnesium by plasma electrolytic oxidation, J. Mater. Sci., 43 (2008) 1532-1538.

[49] E. Matykina, R. Arrabal, P. Skeldon, G.E. Thompson, Investigation of the growth processes of coatings formed by AC plasma electrolytic oxidation of aluminium, Electrochim. Acta, 54 (2009) 6767-6778.

[50] D.-Y. Kim, M. Kim, H.-E. Kim, Y.-H. Koh, H.-W. Kim, J.-H. Jang, Formation of hydroxyapatite within porous TiO2 layer by micro-arc oxidation coupled with electrophoretic deposition, Acta Biomater., 5 (2009) 2196-2205.

[51] K.R. Shin, S.I.I. Yoon, H.W. Yang, Y.G. Ko, D.H. Shin, Formation of β-tricalcium phosphate coating layer on titanium via micro-arc oxidation, Mater. Res. Innov., 18 (2014) S2-997-S992-1000.

[52] Y. Bai, I.S. Park, S.J. Lee, T.S. Bae, W. Duncan, M. Swain, M.H. Lee, One-step approach for hydroxyapatite-incorporated TiO2 coating on titanium via a combined technique of micro-arc oxidation and electrophoretic deposition, Appl. Surf. Sci., 257 (2011) 7010-7018.

[53] J.-H. Lee, H.-E. Kim, Y.-H. Koh, Highly porous titanium (Ti) scaffolds with bioactive microporous hydroxyapatite/TiO2 hybrid coating layer, Mater. Lett., 63 (2009) 1995-1998.

[54] X. Lu, C. Blawert, M.L. Zheludkevich, K.U. Kainer, Insights into plasma electrolytic oxidation treatment with particle addition, Corros. Sci., 101 (2015) 201-207.

[55] X. Lu, C. Blawert, K.U. Kainer, M.L. Zheludkevich, Investigation of the formation mechanisms of plasma electrolytic oxidation coatings on Mg alloy AM50 using particles, Electrochim. Acta, 196 (2016) 680-691.

[56] W.K. Yeung, I.V. Sukhorukova, D.V. Shtansky, E.A. Levashov, I.Y. Zhitnyak, N.A. Gloushankova, P.V. Kiryukhantsev-Korneev, M.I. Petrzhik, A. Matthews, A. Yerokhin, Characteristics and in vitro response of thin hydroxyapatite-titania films produced by plasma electrolytic oxidation of Ti alloys in electrolytes with particle additions, RSC Adv., 6 (2016) 12688-12698.

[57] C. Blawert, S.P. Sah, J. Liang, Y. Huang, D. Höche, Role of sintering and clay particle additions on coating formation during PEO processing of AM50 magnesium alloy, Surf. Coat. Technol., 213 (2012) 48-58.

[58] G. Rapheal, S. Kumar, N. Scharnagl, C. Blawert, Effect of current density on the microstructure and corrosion properties of plasma electrolytic oxidation (PEO) coatings on AM50 Mg alloy produced in an electrolyte containing clay additives, Surf. Coat. Technol., 289 (2016) 150-164.

[59] R. Arrabal, M. Mohedano, E. Matykina, A. Pardo, B. Mingo, M.C. Merino, Characterization and wear behaviour of PEO coatings on 6082-T6 aluminium alloy with incorporated α-Al2O3 particles, Surf. Coat. Technol., 269 (2015) 64-73.

[60] X. Lu, S.P. Sah, N. Scharnagl, M. Störmer, M. Starykevich, M. Mohedano, C. Blawert, M.L. Zheludkevich, K.U. Kainer, Degradation behavior of PEO coating on AM50 magnesium alloy produced from electrolytes with clay particle addition, Surf. Coat. Technol., 269 (2015) 155-169.

[61] M. Mohedano, C. Blawert, M.L. Zheludkevich, Silicate-based Plasma Electrolytic Oxidation (PEO) coatings with incorporated CeO2 particles on AM50 magnesium alloy, Mater. Des., 86 (2015) 735-744.

[62] D. Zhang, Y. Gou, Y. Liu, X. Guo, A composite anodizing coating containing superfine Al2O3 particles on AZ31 magnesium alloy, Surf. Coat. Technol., 236 (2013) 52-57.

[63] C. Ma, M. Zhang, Y. Yuan, X. Jing, X. Bai, Tribological behavior of plasma electrolytic oxidation coatings on the surface of Mg8Li1Al alloy, Tribol. Inter., 47 (2012) 62-68.

[64] Y.M. Wang, F.H. Wang, M.J. Xu, B. Zhao, L.X. Guo, J.H. Ouyang, Microstructure and corrosion behavior of coated AZ91 alloy by microarc oxidation for biomedical application, Appl. Surf. Sci., 255 (2009) 9124-9131.

[65] M. Daroonparvar, M.A.M. Yajid, N.M. Yusof, H.R. Bakhsheshi-Rad, Preparation and corrosion resistance of a nanocomposite plasma electrolytic oxidation coating on Mg-1%Ca alloy formed in aluminate electrolyte containing titania nano-additives, J. Alloy. Compd., 688, Part A (2016) 841-857.

[66] Y.L. Song, X.Y. Sun, Y.H. Liu, Effect of TiO2 nanoparticles on the microstructure and corrosion behavior of MAO coatings on magnesium alloy, Mater. Corros., 63 (2012) 813-818.

[67] P.B. Srinivasan, J. Liang, C. Blawert, M. Störmer, W. Dietzel, Development of decorative and corrosion resistant plasma electrolytic oxidation coatings on AM50 magnesium alloy, Surf. Eng., 26 (2010) 367-370.

[68] M. Tang, H. Liu, W. Li, L. Zhu, Effect of zirconia sol in electrolyte on the characteristics of microarc oxidation coating on AZ91D magnesium, Mater. Lett., 65 (2011) 413-415.

[69] D. Sreekanth, N. Rameshbabu, Development and characterization of MgO/hydroxyapatite composite coating on AZ31 magnesium alloy by plasma electrolytic oxidation coupled with electrophoretic deposition, Mater. Lett., 68 (2012) 439-442.

[70] X. Lin, X. Wang, L. Tan, P. Wan, X. Yu, Q. Li, K. Yang, Effect of preparation parameters on the properties of hydroxyapatite containing micro-arc oxidation coating on biodegradable ZK60 magnesium alloy, Ceram. Inter., 40 (2014) 10043-10051.

[71] X. Lu, C. Blawert, N. Scharnagl, K.U. Kainer, Influence of incorporating Si3N4 particles into the oxide layer produced by plasma electrolytic oxidation on AM50 Mg alloy on coating morphology and corrosion properties, J. Magnesium Alloy., 1 (2013) 267-274.

[72] L. Yu, J. Cao, Y. Cheng, An improvement of the wear and corrosion resistances of AZ31 magnesium alloy by plasma electrolytic oxidation in a silicate–hexametaphosphate electrolyte with the suspension of SiC nanoparticles, Surf. Coat. Technol., 276 (2015) 266-278.

[73] X. Ma, S. Zhu, L. Wang, C. Ji, C. Ren, S. Guan, Synthesis and properties of a bio-composite coating formed on magnesium alloy by one-step method of micro-arc oxidation, J. Alloy. Compd., 590 (2014) 247-253.

[74] Y.Q. Wang, M.Y. Zheng, K. Wu, Microarc oxidation coating formed on SiCw/AZ91 magnesium matrix composite and its corrosion resistance, Mater. Lett., 59 (2005) 1727-1731.

[75] R. Arrabal, E. Matykina, P. Skeldon, G.E. Thompson, Coating formation by plasma electrolytic oxidation on ZC71/SiC/12p-T6 magnesium metal matrix composite, Appl. Surf. Sci., 255 (2009) 5071-5078.

[76] W. Xue, Q. Jin, Q. Zhu, M. Hua, Y. Ma, Anti-corrosion microarc oxidation coatings on SiCP/AZ31 magnesium matrix composite, J. Alloy. Compd., 482 (2009) 208-212.

[77] R. Arrabal, A. Pardo, M.C. Merino, M. Mohedano, P. Casajús, E. Matykina, P. Skeldon, G.E. Thompson, Corrosion behaviour of a magnesium matrix composite with a silicate plasma electrolytic oxidation coating, Corros. Sci., 52 (2010) 3738-3749.

[78] M.Q. Tang, W.P. Li, H.C. Liu, L.Q. Zhu, The effect of titania sol in phosphate electrolyte on microarc oxidation coatings on aluminum alloy, Inter. J. Mod. Phys. B, 24 (2010) 3190-3195.

[79] A. Bahramian, K. Raeissi, A. Hakimizad, An investigation of the characteristics of Al2O3/TiO2 PEO nanocomposite coating, Appl. Surf. Sci., 351 (2015) 13-26.

[80] H.-x. Li, R.-g. Song, Z.-g. Ji, Effects of nano-additive TiO2 on performance of micro-arc oxidation coatings formed on 6063 aluminum alloy, Trans. Nonferrous Met. Soc. China, 23 (2013) 406-411.

[81] P. Wang, J. Li, Y. Guo, J. Wang, Z. Yang, M. Liang, The formation mechanism of the composited ceramic coating with thermal protection feature on an Al12Si piston alloy via a modified PEO process, J. Alloy. Compd., 682 (2016) 357-365.

[82] V.N. Malyshev, K.M. Zorin, Features of microarc oxidation coatings formation technology in slurry electrolytes, Appl. Surf. Sci., 254 (2007) 1511-1516.

[83] C.-J. Hu, M.-H. Hsieh, Preparation of ceramic coatings on an Al–Si alloy by the incorporation of ZrO2 particles in microarc oxidation, Surf. Coat. Technol., 258 (2014) 275-283.

[84] F. Jin, P.K. Chu, H. Tong, J. Zhao, Improvement of surface porosity and properties of alumina films by incorporation of Fe micrograins in micro-arc oxidation, Appl. Surf. Sci., 253 (2006) 863-868.

[85] Y. Yürektürk, F. Muhaffel, M. Baydoğan, Characterization of micro arc oxidized 6082 aluminum alloy in an electrolyte containing carbon nanotubes, Surf. Coat. Technol., 269 (2015) 83-90.

[86] Y.S. Kim, H.W. Yang, K.R. Shin, Y.G. Ko, D.H. Shin, Heat dissipation properties of oxide layers formed on 7075 Al alloy via plasma electrolytic oxidation, Surf. Coat. Technol., 269 (2015) 114-118.

[87] X. Wu, W. Qin, Y. Guo, Z. Xie, Self-lubricative coating grown by micro-plasma oxidation on aluminum alloys in the solution of aluminate–graphite, Appl. Surf. Sci., 254 (2008) 6395-6399.

[88] Y. Yang, Y. Liu, Effects of Current Density on the Microstructure and the Corrosion Resistance of Alumina Coatings Embedded with SiC Nano-particles Produced by Micro-arc Oxidation, J. Mater. Sci. Technol., 26 (2010) 1016-1020.

[89] K.-J. Ma, M.M.S. Al Bosta, W.-T. Wu, Preparation of self-lubricating composite coatings through a micro-arc plasma oxidation with graphite in electrolyte solution, Surf. Coat. Technol., 259, Part B (2014) 318-324.

[90] M. Mu, J. Liang, X. Zhou, Q. Xiao, One-step preparation of TiO2/MoS2 composite coating on Ti6Al4V alloy by plasma electrolytic oxidation and its tribological properties, Surf. Coat. Technol., 214 (2013) 124-130.

[91] X.-q. Wu, F.-q. Xie, Z.-c. Hu, L. Wang, Effects of additives on corrosion and wear resistance of micro-arc oxidation coatings on TiAl alloy, Trans. Nonferrous Met. Soc. China, 20 (2010) 1032-1036.

[92] S. Sarbishei, M.A. Faghihi Sani, M.R. Mohammadi, Study plasma electrolytic oxidation process and characterization of coatings formed in an alumina nanoparticle suspension, Vacuum, 108 (2014) 12-19.

[93] M. Aliofkhazraei, R.S. Gharabagh, M. Teimouri, M. Ahmadzadeh, G.B. Darband, H. Hasannejad, Ceria embedded nanocomposite coating fabricated by plasma electrolytic oxidation on titanium, J. Alloy. Compd., 685 (2016) 376-383.

[94] M.S. Vasil'eva, V.S. Rudnev, I.A. Korotenko, A.Y. Ustinov, Producing and investigating oxide coatings containing manganese and nickel compounds on titanium from electrolyte suspensions, Prot. Met. Phys. Chem. Surf., 46 (2010) 593-598.

[95] X. Yao, X. Zhang, H. Wu, L. Tian, Y. Ma, B. Tang, Microstructure and antibacterial properties of Cu-doped TiO2 coating on titanium by micro-arc oxidation, Appl. Surf. Sci., 292 (2014) 944-947.

[96] M. Mu, X. Zhou, Q. Xiao, J. Liang, X. Huo, Preparation and tribological properties of self-lubricating TiO2/graphite composite coating on Ti6Al4V alloy, Appl. Surf. Sci., 258 (2012) 8570-8576.

[97] F. Samanipour, M.R. Bayati, F. Golestani-Fard, H.R. Zargar, A.R. Mirhabibi, V. Shoaei-Rad, S. Abbasi, Innovative fabrication of ZrO2–HAp–TiO2 nano/micro-structured composites through MAO/EPD combined method, Mater. Lett., 65 (2011) 926-928.

[98] X. Jiang, Y. Wang, C. Pan, Micro-arc oxidation of TC4 substrates to fabricate TiO2/YAG:Ce3+ compound films with enhanced photocatalytic activity, J. Alloy. Compd., 509 (2011) L137-L141.

[99] E. Matykina, M. Montuori, J. Gough, F. Monfort, A. Berkani, P. Skeldon, G.E. Thompson, H. Habazaki, Spark anodising of titanium for biomedical applications, Trans. IMF, 84 (2006) 125-133.

[100] P. Whiteside, E. Matykina, J.E. Gough, P. Skeldon, G.E. Thompson, In vitro evaluation of cell proliferation and collagen synthesis on titanium following plasma electrolytic oxidation, J. Biomed. Mater. Res. A, 94a (2010) 38-46.

[101] M. Mohedano, R. Guzman, R. Arrabal, J.L. Lacomba, E. Matykina, Bioactive plasma electrolytic oxidation coatings-The role of the composition, microstructure, and electrochemical stability, J. Biomed. Mater. Res. B, 101 (2013) 1524-1537.

[102] M. Mohedano, E. Matykina, R. Arrabal, A. Pardo, M.C. Merino, Metal release from ceramic coatings for dental implants, Dent. Mater., 30 (2014) E28-E40.

[103] H. Cimenoglu, M. Gunyuz, G.T. Kose, M. Baydogan, F. Uğurlu, C. Sener, Micro-arc oxidation of Ti6Al4V and Ti6Al7Nb alloys for biomedical applications, Mater. Charact., 62 (2011) 304-311.

[104] Y. Yang, H. Wu, Effects of Current Frequency on the Microstructure and Wear Resistance of Ceramic Coatings Embedded with SiC Nano-particles Produced by Micro-arc Oxidation on AZ91D Magnesium Alloy, J. Mater. Sci. Technol., 26 (2010) 865-871.

[105] R. Balaji, M. Pushpavanam, K.Y. Kumar, K. Subramanian, Electrodeposition of bronze-PTFE composite coatings and study on their tribological characteristics, Surf. Coat. Tech., 201 (2006) 3205-3211.

[106] Y.-K. Shin, W.-S. Chae, Y.-W. Song, Y.-M. Sung, Formation of titania photocatalyst films by microarc oxidation of Ti and Ti–6Al–4V alloys, Electrochem. Commun., 8 (2006) 465-470.

[107] Y.S. Zhong, X.D. He, L.P. Shi, M.W. Li, F. He, Tailored Al2O3/ZrO2 Composite Oxide Layers by Bipolar Current Adjustment in the Plasma Electrolytic Oxidation (PEO) Process, Nanosci. Nanotechnol. Lett., 3 (2011) 209-214.

[108] Q. Luo, Q.-z. Cai, X.-w. Li, Z.-h. Pan, Y.-j. Li, X.-d. Chen, Q.-s. Yan, Preparation and characterization of ZrO2/TiO2 composite photocatalytic film by micro-arc oxidation, Trans. Nonferrous Met. Soc. China, 23 (2013) 2945-2950.

[109] T. Soejima, H. Yagyu, S. Ito, One-pot synthesis and photocatalytic activity of Fe-doped TiO2 films with anatase–rutile nanojunction prepared by plasma electrolytic oxidation, J. Mater. Sci., 46 (2011) 5378-5384.

[110] V.S. Rudnev, M.V. Adigamova, I.V. Lukiyanchuk, A.Y. Ustinov, I.A. Tkachenko, P.V. Kharitonskii, A.M. Frolov, V.P. Morozova, The effect of the conditions of formation on ferromagnetic properties of iron-containing oxide coatings on titanium, Prot. Met. Phys. Chem. Surf., 48 (2012) 543-552.

[111] S.V. Gnedenkov, S.L. Sinebryukhov, I.A. Tkachenko, D.V. Mashtalyar, A.Y. Ustinov, A.V. Samokhin, Y.V. Tsvetkov, Magnetic properties of surface layers formed on titanium by plasma electrolytic oxidation, Inorg. Mater. Appl. Res., 3 (2012) 151-156.

[112] Y. Bai, K.-A. Kim, I.S. Park, S.J. Lee, T.S. Bae, M.H. Lee, In situ composite coating of titania–hydroxyapatite on titanium substrate by micro-arc oxidation coupled with electrophoretic deposition processing, Mater. Sci. Eng. B, 176 (2011) 1213-1221.

[113] Y. Bai, I.S. Park, H.H. Park, T.S. Bae, M.H. Lee, Formation of bioceramic coatings containing hydroxyapatite on the titanium substrate by micro-arc oxidation coupled with electrophoretic deposition, J. Biomed. Mater. Res. B, 95B (2010) 365-373.

[114] K.R. Shin, Y.G. Ko, D.H. Shin, Influence of zirconia on biomimetic apatite formation in pure titanium coated via plasma electrolytic oxidation, Mater. Lett., 64 (2010) 2714-2717.

[115] K.R. Shin, Y.G. Ko, D.H. Shin, Surface characteristics of ZrO2-containing oxide layer in titanium by plasma electrolytic oxidation in K4P2O7 electrolyte, J. Alloy. Compd., 536 (2012) S226-S230.

[116] K.R. Shin, Y.S. Kim, G.W. Kim, Y.G. Ko, D.H. Shin, Development of titanium oxide layer containing nanocrystalline zirconia particles with tetragonal structure: Structural and biological characteristics, Colloid. Surface B, 131 (2015) 47-53.

[117] B.S. Atiyeh, M. Costagliola, S.N. Hayek, S.A. Dibo, Effect of silver on burn wound infection control and healing: Review of the literature, Burns, 33 (2007) 139-148.

[118] D. Teker, F. Muhaffel, M. Menekse, N.G. Karaguler, M. Baydogan, H. Cimenoglu, Characteristics of multi-layer coating formed on commercially pure titanium for biomedical applications, Mater. Sci. Eng. C, 48 (2015) 579-585.

[119] K.J.L. Burg, S. Porter, J.F. Kellam, Biomaterial developments for bone tissue engineering, Biomater., 21 (2000) 2347-2359.

[120] R.H.J. Hannink, Microstructural Development of Sub-Eutectoid Aged MgO-ZrO2 Alloys, J. Mater. Sci., 18 (1983) 457-470.

[121] O. Fukumasa, R. Tagashira, K. Tachino, H. Mukunoki, Spraying of MgO films with a well-controlled plasma jet, Surf. Coat. Tech., 169 (2003) 579-582.

[122] P. Galliano, J.J. De Damborenea, M.J. Pascual, A. Duran, Sol-gel coatings on 316L steel for clinical applications, J. Sol-Gel Sci. Techn., 13 (1998) 723-727.

[123] D.C.L. Vasconcelos, J.A.N. Carvalho, M. Mantel, W.L. Vasconcelos, Corrosion resistance of stainless steel coated with sol-gel silica, J. Non-Cryst. Solids, 273 (2000) 135-139.

[124] D. Wang, G.P. Bierwagen, Sol–gel coatings on metals for corrosion protection, Prog. Org. Coat., 64 (2009) 327-338.

[125] M.A. Khazrayie, A.R.S. Aghdam, Si3N4/Ni nanocomposite formed by electroplating: Effect of average size of nanoparticulates, Trans. Nonferrous Met. Soc. China, 20 (2010) 1017-1023.

[126] A. Pepe, M. Aparicio, A. Durán, S. Ceré, Cerium hybrid silica coatings on stainless steel AISI 304 substrate, J. Sol-Gel Sci. Techn., 39 (2006) 131-138.

[127] M. Schem, T. Schmidt, J. Gerwann, M. Wittmar, M. Veith, G.E. Thompson, I.S. Molchan, T. Hashimoto, P. Skeldon, A.R. Phani, S. Santucci, M.L. Zheludkevich, CeO2-filled sol–gel coatings for corrosion protection of AA2024-T3 aluminium alloy, Corros. Sci., 51 (2009) 2304-2315.

[128] R.T. Bhatt, S.R. Choi, L.M. Cosgriff, D.S. Fox, K.N. Lee, Impact resistance of environmental barrier coated SiC/SiC composites, Mater. Sci. Eng. A, 476 (2008) 8-19.

[129] C. Czosnek, M.M. Bućko, J.F. Janik, Z. Olejniczak, M. Bystrzejewski, O. Łabędź, A. Huczko, Preparation of silicon carbide SiC-based nanopowders by the aerosol-assisted synthesis and the DC thermal plasma synthesis methods, Mater. Res. Bull., 63 (2015) 164-172.

[130] Y.-Q. Hou, D.-M. Zhuang, G. Zhang, M.-S. Wu, J.-J. Liu, Tribological performances of diamond film and graphite/diamond composite film, Wear, 253 (2002) 711-719.

[131] S. Dorozhkin, Calcium Orthophosphates in Nature, Biology and Medicine, Mater., 2 (2009) 399.

[132] V.S. Rudnev, I.V. Lukiyanchuk, M.V. Adigamova, V.P. Morozova, I.A. Tkachenko, The effect of nanocrystallites in the pores of PEO coatings on their magnetic properties, Surf. Coat. Technol., 269 (2015) 23-29.

[133] R.Q. Hang, A. Gao, X.B. Huang, X.G. Wang, X.Y. Zhang, L. Qin, B. Tang, Antibacterial activity and cytocompatibility of Cu-Ti-O nanotubes, J. Biomed. Mater. Res. A, 102 (2014) 1850-1858.

Table 1 Particles applied in PEO processing

Particles	Properties and field of applications	Reference
Polytetrafluoroethylene (PTFE)	Lower friction coefficient, chemical inertness and hydrophobicity	[105]
Ag	Antibacterial activity	[117]
Hydroxyapatite (HA)	Osteogenesis and biomaterial	[119]
MoS_2	Solid lubricant	[90]
Clay minerals	Absorption capacities and filler material	[57]
ZrO_2 (monoclinic, tetragonal, and cubic)	High chemical stability	[120, 121]
SiO_2	High heat and chemical resistance	[122, 123]
TiO_2	High chemical stability and heat resistance	[124]
Si_3N_4	High hardness and wear resistance	[125]
Al_2O_3	High hardness and insulator	[124]
CeO_2/Ce_2O_3	High chemical stability, superconductors and sensors	[126, 127]
SiC	High mechanical strength and chemical inertness	[128, 129]
Graphite	Solid lubricant	[130]
Calcium phosphates	Natural bone component	[131]
Fe/Fe_2O_3	Ferromagnetic material	[109]
Co	Ferromagnetic material	[132]
Cu	Antibacterial activity	[133]
Ni/NiO, MnO_2/Mn_2O_3	Catalytic activity	[94]

Figure captions

Figure 1 Zeta potentials of ZrO_2 and TiO_2 powders at different pH levels in alkaline fluoride based electrolyte [19].

Figure 2 Voltage-time response of coatings produced from aluminate based electrolyte with and without 10 g/L Al_2O_3 particles on AM60B Mg alloy [26].

Figure 3 The conductivity of an 1.0 M Na_2SiO_3 electrolyte with varied concentration of silica sol at (a) 20 °C; (b) 60 °C [40].

Figure 4 Schematic diagram of the uptake and incorporation mechanism of particles into PEO coating [30].

Figure 5 Overview of the scope, size and incorporation mode of the particles for Mg, Al and Ti alloys.

Figure 6 TEM micrographs and corresponding diffraction pattern from various regions of the coating with clay particle addition (a) top surface region, (b) center region and (c) interface region [57].

Figure 7 Surface morphologies of oxide film formed in an alkaline phosphate bath without (a) and with (b) addition of 4 vol% titania sol [23].

Figure 8 XRD patterns for (a) SiCP/AZ31 composite substrate, (b) 30 μm coating, and (c) 80 μm coating [76].

Figure 9 Ti6Al4V coated in constant voltage bipolar regime (A-anatase, R-rutile, HA-hydroxyapatite) [103].

Figure 10 Wear tracks (a) coating with Al_2O_3 nanoparticles, (b) coating without Al_2O_3 nanoparticles and (c) AZ31 substrate [62].

Figure 11 Vickers hardness of the substrate and PEO coatings with different concentrations of Al_2O_3 nanoparticles [29].

Figure 12 (a, b) Nyquist and (c) Bode plots of pure PEO, composite films and bare magnesium alloy [47].

Figure 13 Apatite forming ability of (a) PEO and (b) PEO incorporated with particles after immersion in SBF for 3 days [47].

Figure 14 Surface appearance of bare Mg and PEO coatings with different amount of titania sol after the immersion tests in SBF solution for different time period (arrows indicating the corrosion sites) [64].

Figure 15 The decomposition rate of Methylthionine blue (MB) (a) blank solution, (b) MB + Mg alloy with PEO coating formed in the base electrolyte and (c) MB + samples with PEO coating formed in the electrolyte with 4 g/L TiO_2 nanoparticles [28].

Figure 16 Hardness profiles of PEO coatings on 6082 Al alloy with and without α-Al_2O_3 particles [59].

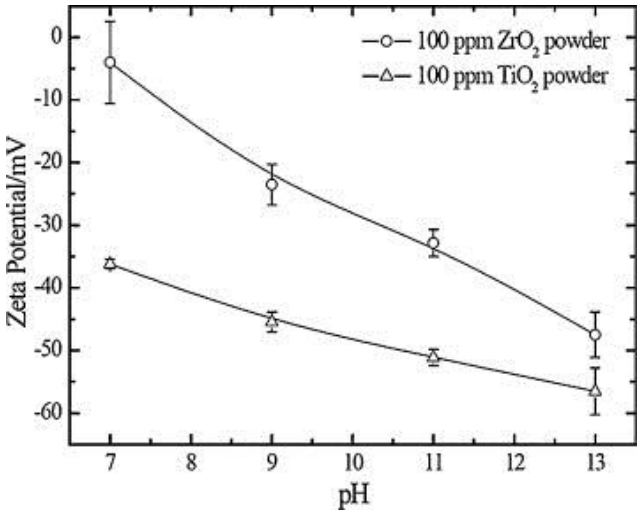

Figure 1

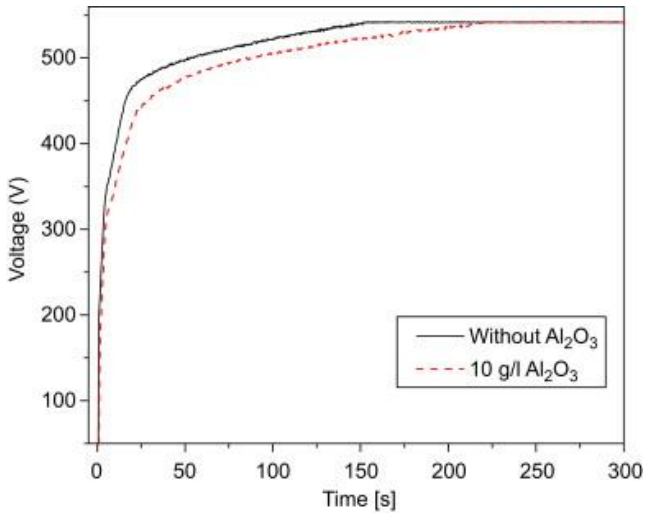

Figure 2

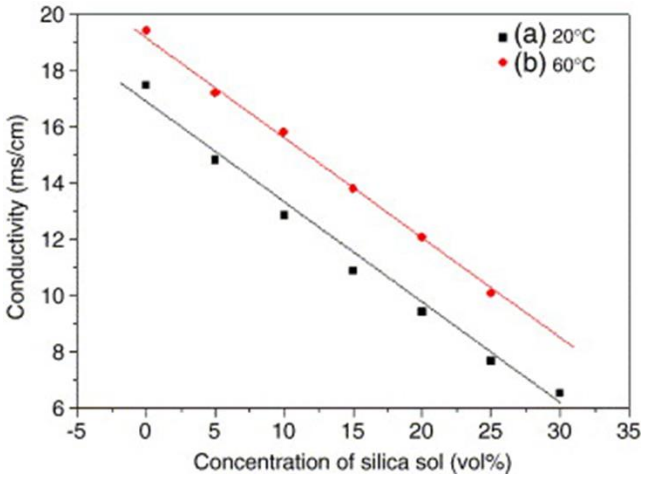

Figure 3

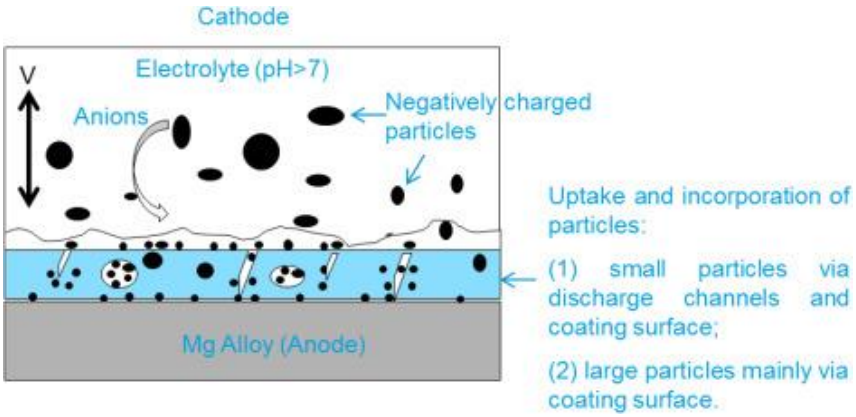

Figure 4

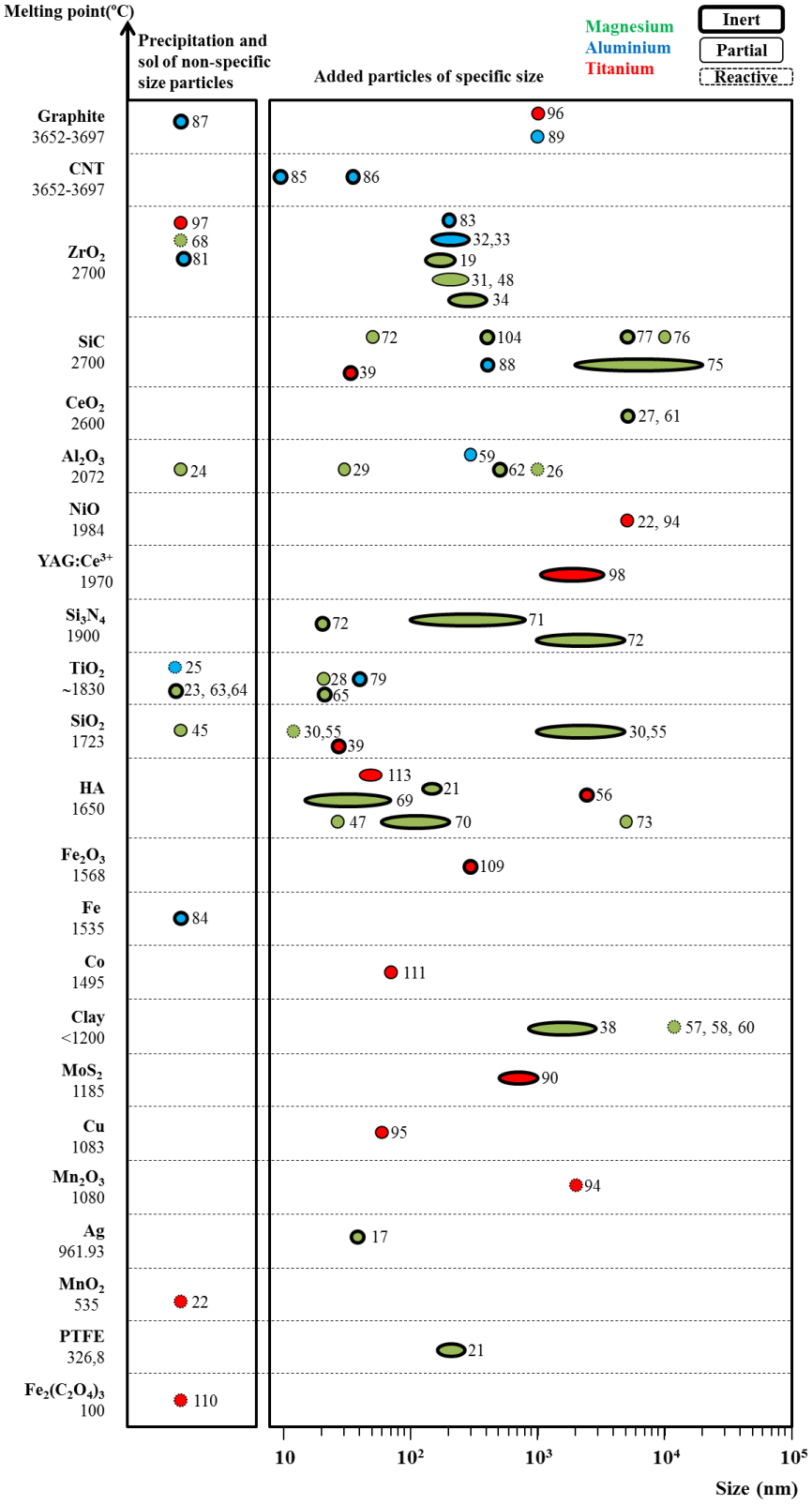
Melting point(°C)
Precipitation and sol of non-specific size particles
Added particles of specific size
Magnesium
Aluminium
Titanium
Inert
Partial
Reactive
Graphite 3652-3697
CNT 3652-3697
ZrO2 2700
SiC 2700
CeO2 2600
Al2O3 2072
NiO 1984
YAG:Ce3+ 1970
Si3N4 1900
TiO2 ~1830
SiO2 1723
HA 1650
Fe2O3 1568
Fe 1535
Co 1495
Clay <1200
MoS2 1185
Cu 1083
Mn2O3 1080
Ag 961.93
MnO2 535
PTFE 326,8
Fe2(C2O4)3 100
10
10²
10³
10⁴
10⁵
Size (nm)

Figure 5

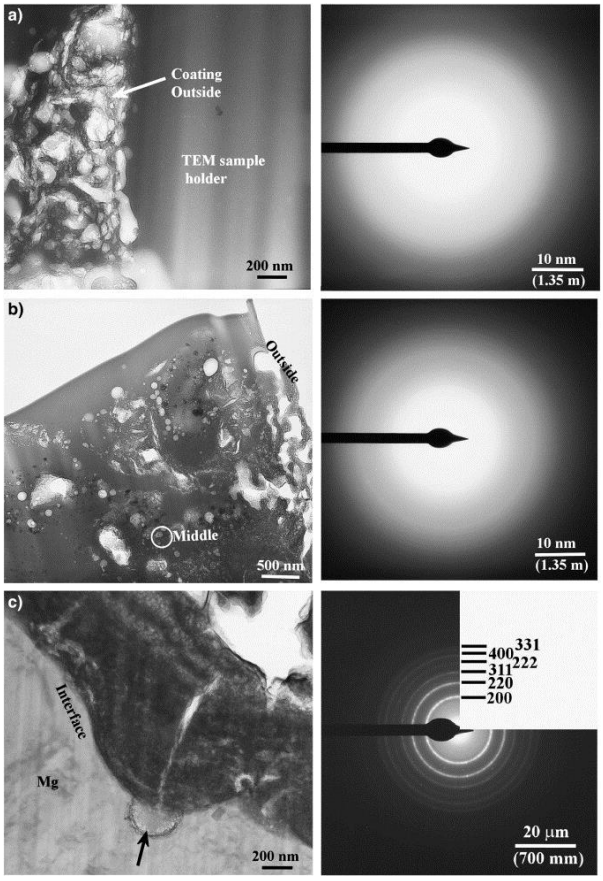

Figure 6

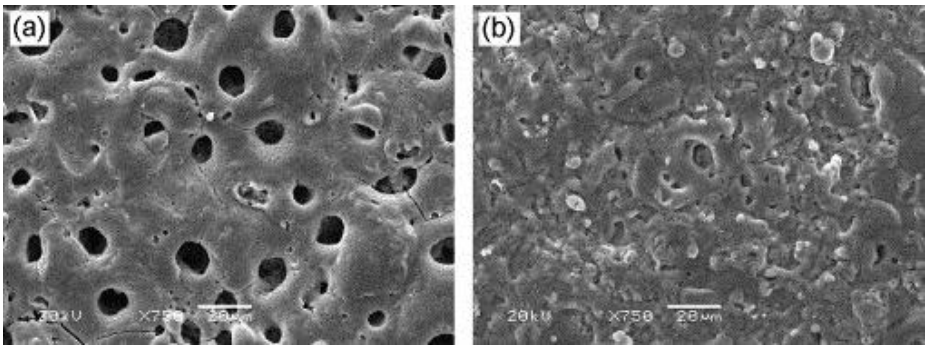

Figure 7

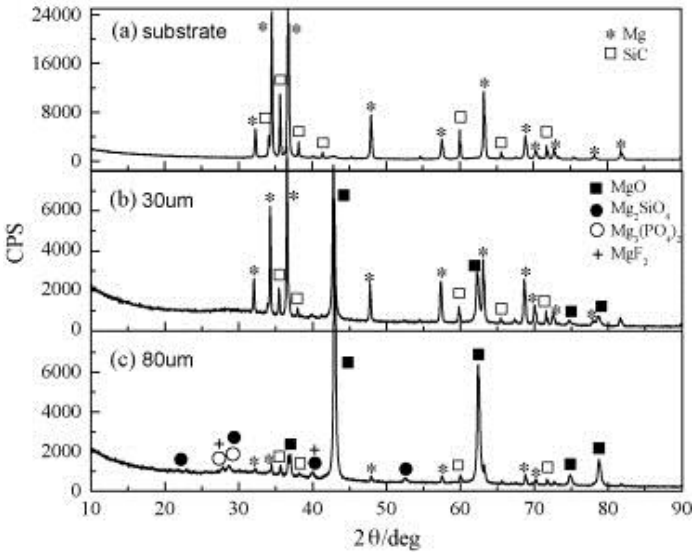

Figure 8

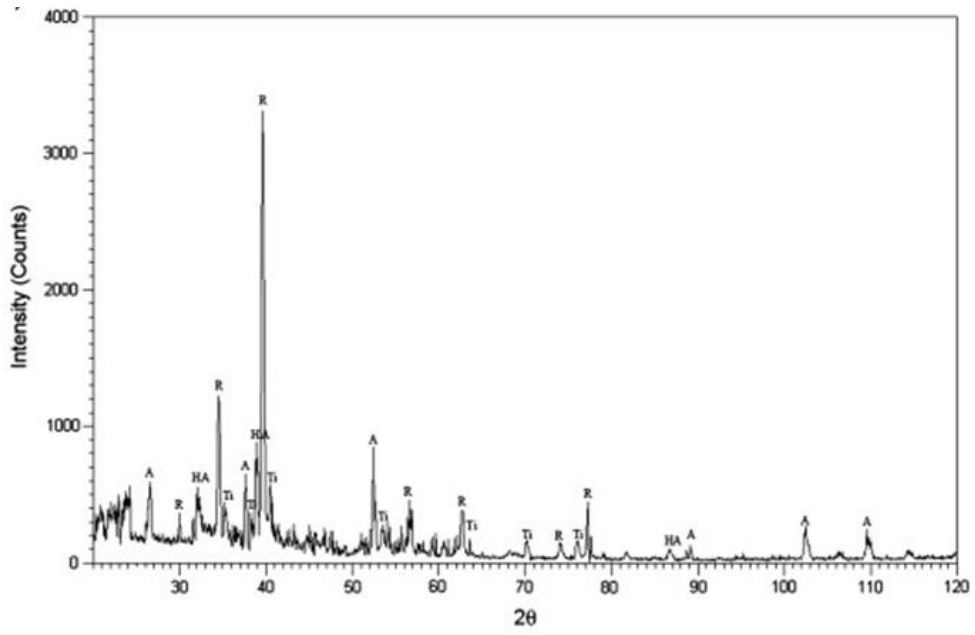

Figure 9

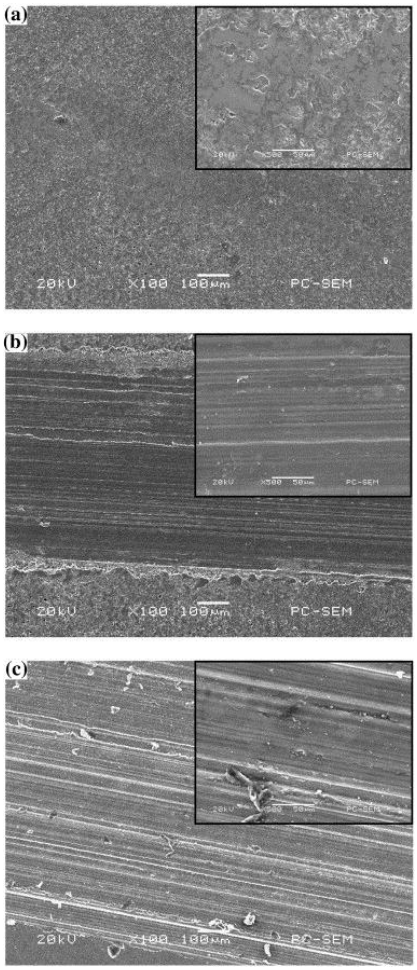

Figure 10

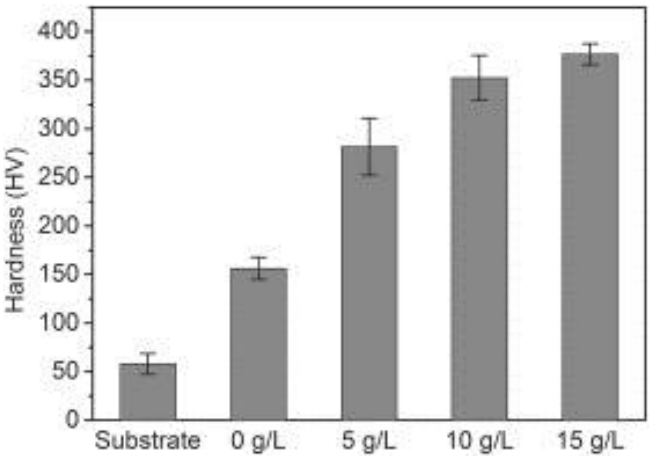

Figure 11

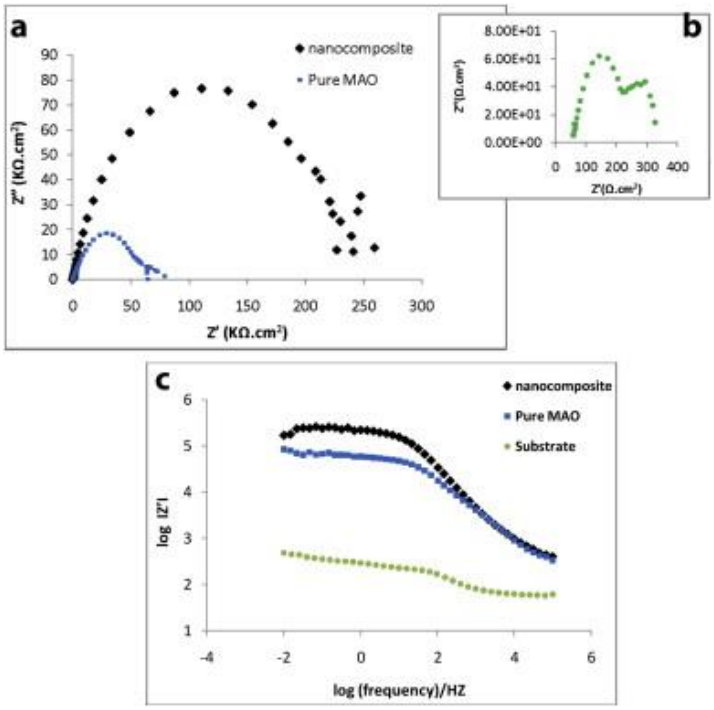

Figure 12

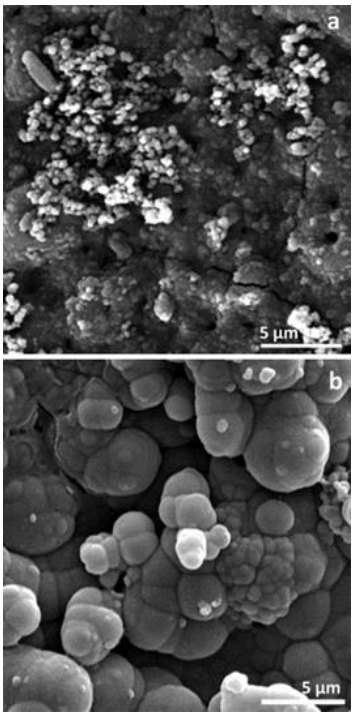

Figure 13

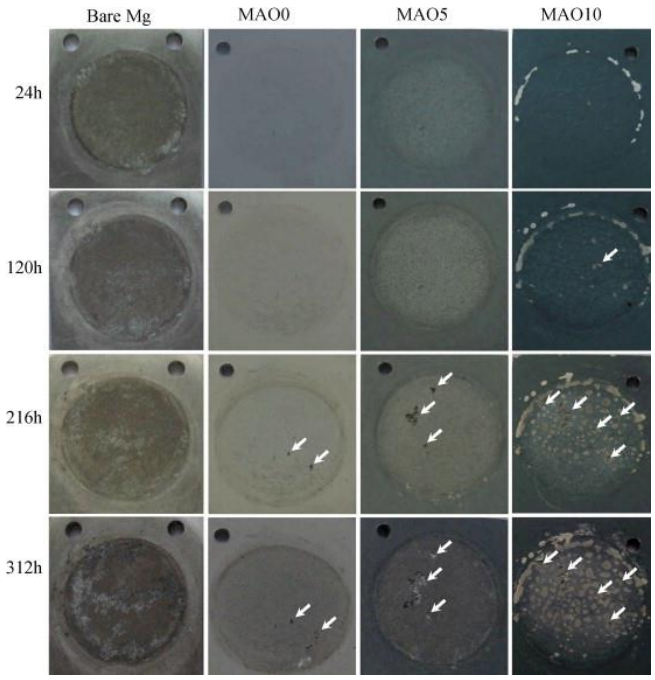

Figure 14

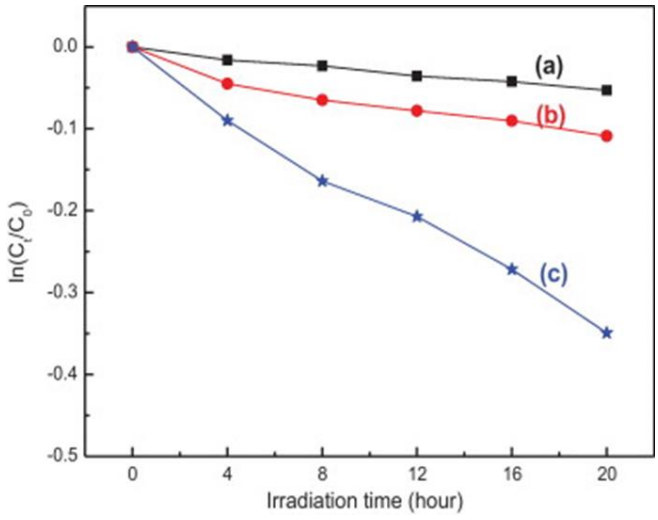

Figure 15

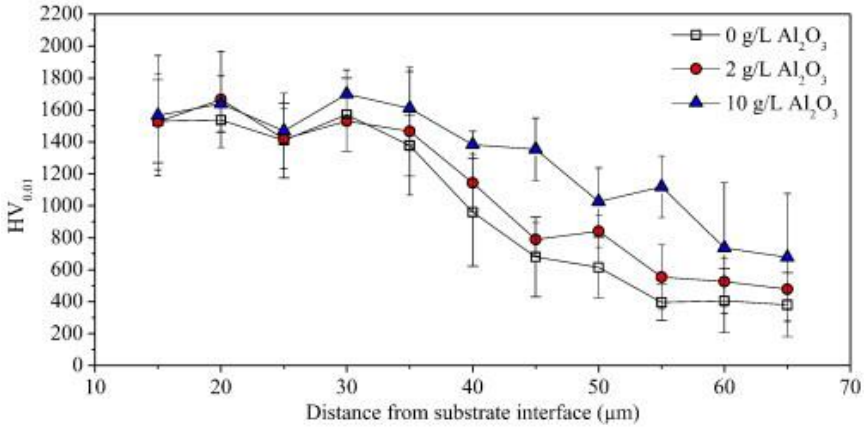

Figure 16

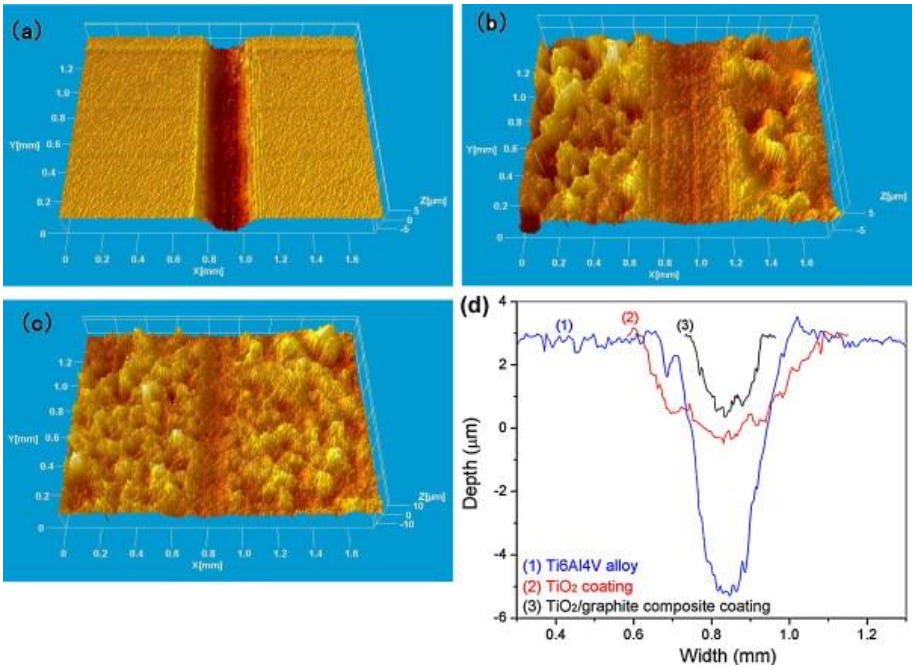

Figure 17

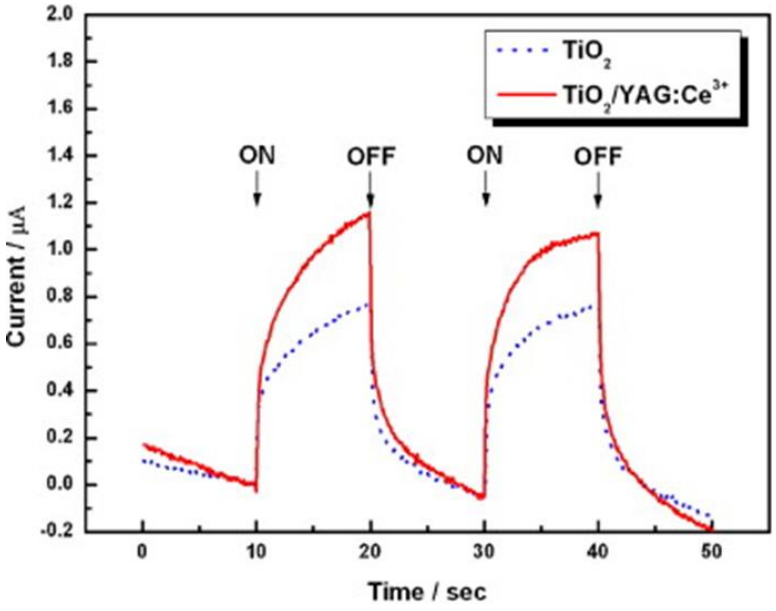

Figure 18

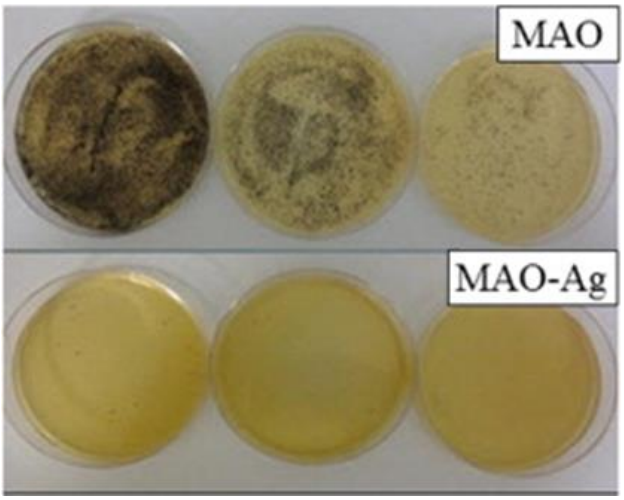

Figure 19